arXiv:0810.1016v2 [hep-ph] 31 Oct 2008

October 31, 2008
UMD-PP-08-015

Flavor Violation Tests of Warped/Composite SM in the Two-Site Approach

Kaustubh Agashe , Aleksandr Azatov and Lijun Zhu

Maryland Center for Fundamental Physics, Department of Physics, University of Maryland,
College Park, MD 20742, USA

Abstract

We study flavor violation in the quark sector in a purely $4D$, two-site effective field theory description of the Standard Model and just their first Kaluza-Klein excitations from a warped extra dimension. The warped $5D$ framework can provide solutions to both the Planck-weak and flavor hierarchies of the SM. It is also related (via the AdS/CFT correspondence) to partial compositeness of the SM. We focus on the dominant contributions in the two-site model to two observables which we argue provide the strongest constraints from flavor violation, namely, ϵ_K and BR $(b \to s\gamma)$, where contributions in the two-site model occur at tree and loop-level, respectively. In particular, we demonstrate that a "tension" exists between these two observables in the sense that they have opposite dependence on composite site Yukawa couplings, making it difficult to decouple flavor-violating effects using this parameter. We choose the size of the composite site QCD coupling based on the relation of the two-site model to the $5D$ model (addressing the Planck-weak hierarchy), where we match the $5D$ QCD coupling to the $4D$ coupling at the loop-level and assuming negligible tree-level brane-localized kinetic terms. We estimate that a larger size of the $5D$ gauge coupling is constrained by the requirement of $5D$ perturbativity. We find that $\sim O(5)$ TeV mass scale for the new particles in the two-site model can then be consistent with both observables. We also compare our analysis of ϵ_K in the two-site model to that in $5D$ models, including both the cases of a brane-localized and bulk Higgs.

1 Introduction

The framework of a warped extra dimension with Standard Model (SM) fields propagating in the bulk [1, 2, 3] is a very attractive extension of the SM since it can provide solutions to both the Planck-weak [4] and flavor hierarchy problems of the SM [2, 3]. Moreover, the versions of this framework with a grand unified gauge symmetry in the bulk can naturally lead to precision unification of the three SM gauge couplings [5] and a candidate for the dark matter of the universe (the latter from requiring longevity of the proton) [6]. The new particles in this framework are the Kaluza-Klein (KK) excitations of the SM fields with mass at the $\sim$ TeV scale. Such a framework can thus give significant contributions to various precision tests of the SM. The electroweak precision tests (EWPT) can be satisfied for KK mass scale of a few TeV [7, 8, 9] using suitable custodial symmetries [7, 10].

In this paper, we focus on the solution to the flavor hierarchy of the SM in the framework of warped extra dimension and the resulting flavor-violation. The idea is that the effective $4D$ Yukawa couplings of the SM fermions are given by a product of the fundamental $5D$ Yukawa couplings and the overlap of the profiles (of the SM fermions and the Higgs) in the extra dimension. Moreover, vastly different profiles in the extra dimension for the SM fermions (which are the zero-modes of $5D$ fermions), and hence their hierarchical overlaps with Higgs, can be easily obtained by small variations in the $5D$ fermion mass parameters. Thus, hierarchies in the $4D$ Yukawa couplings can be generated without any (large) hierarchies in the fundamental $5D$ parameters ($5D$ Yukawa couplings and $5D$ mass parameters for fermions). As a corollary, the couplings of SM fermions (with different profiles) to KK modes (again following from the relevant overlaps of profiles) are non-universal, resulting in flavor violation from exchange of these KK modes [11]. However, there is a built-in analog of GIM mechanism of the SM in this framework [3, 12, 13] which suppresses flavor changing neutral currents (FCNC's). Namely, the non-universalities in couplings of SM fermions to KK modes are of the size of $4D$ Yukawa couplings since KK modes have a similar profile to the SM Higgs.

In spite of this analog of the GIM mechanism, it was shown recently [14, 15] (see also [16, 17]) that the constraint on KK mass scale from contributions of KK gluon to ϵ_K is quite stringent. In particular, for the model with the SM Higgs (strictly) localized on the TeV brane in a $5D$ slice of anti-de Sitter space (AdS), the limit on the KK mass scale from ϵ_K is ~ 10 TeV for the smallest allowed $5D$ QCD coupling obtained by *loop*-level matching to the $4D$ coupling with negligible tree-level brane kinetic terms (in the framework which addresses the Planck-weak hierarchy). On the other hand, for larger brane kinetic terms such that the $5D$ QCD coupling (in units of the AdS curvature scale) is $\sim 4\pi$, the lower limit on KK mass scale increases to ~ 40 TeV. In addition, the constraint on the KK mass scale is weakened as the size of the $5D$ Yukawa (in units of the AdS curvature scale) is increased. However, this direction reduces the regime of validity of the $5D$ effective field theory (EFT): the above limits on KK mass scale are for the size of $5D$ Yukawa such that about two KK modes are allowed in the $5D$ EFT.

In the light of these constraints, instead of an "anarchic" approach to flavor in $5D$, i.e., no hierarchies or relations in the various $5D$ flavor parameters, references [16, 18, 19] have proposed imposing $5D$ flavor symmetries in order to relate these parameters and hence to suppress flavor violation. Lower KK mass scales are thereby allowed, improving the fine-tuning in electroweak symmetry breaking (EWSB) and the discovery potential at the Large Hadron Collider (LHC). For other flavor studies in this framework, see references [20, 21, 22, 23, 24].

However, the phenomenology of the TeV-scale KK modes and the SM Higgs is quite sensitive to the structure near the TeV brane (where these particles are localized). For example, the SM Higgs can be the lightest mode of a $5D$ scalar (instead of being a strictly TeV brane-localized field), but with a profile which is still peaked near the TeV brane (such that the Planck-weak hierarchy is still addressed) – we will denote this scenario by "bulk Higgs" [25, 26].[1] Moreover, the warped geometry might deviate from pure AdS near the TeV brane which in fact could be replaced with a "soft wall" [28]. Similarly, in general, there are non-zero TeV brane-localized kinetic terms for the bulk fields [29]. Such variations of the minimal models are not likely to modify the couplings and spectrum of the KK modes/Higgs significantly – for example, the constraint on KK mass scale from various precision tests will not be modified by much more than $O(1)$ factors. However, even such modest changes can dramatically impact the LHC signals, especially the production cross-sections for the KK modes.

Instead of focusing on a *specific* limit of the full $5D$ model, such considerations then strongly motivate analyzing the phenomenology of this framework using a more economical description (for example, using fewer parameters than the $5D$ models) which can capture its robust aspects. Such an approach is provided by the "two site model" [30] which is a purely $4D$ effective field theory obtained by truncating the $5D$ AdS model to the SM particles and their first KK excitations, roughly achieved by "deconstruction/discretization" [31] of the warped extra dimension. Equivalently, based on the AdS/CFT correspondence [32] as applied to a slice of AdS [33], the two-site model also describes two sectors: composites of purely $4D$ strong dynamics and elementary fields (which are not part of the strong dynamics). These two sectors mix, with the resulting mass eigenstates being the SM particles and their heavier partners, which correspond to the zero and KK modes of the $5D$ model. With this motivation in mind, an analysis of EWPT in two-site model was performed in [30].

In this paper, we study flavor-violation in the quark sector in this two-site model, in the incarnation *corresponding to flavor anarchy in the* $5D$ *AdS theory.* We focus on effects of tree-level heavy gluon exchange in ϵ_K and Higgs-heavy fermion loops in BR $(b \to s\gamma)$[2]. We will show that a *combination* of these processes provide the strongest constraints on the two-site model (and hence probably on the general framework of warped extra dimension). We leave a more complete study of flavor violation in the two-site model, including other contributions to these observables and a global analysis (i.e., including other observables), for future work.

---

[1] Note that the models where Higgs is the 5^{th} component of a $5D$ gauge field [27, 8] do *not* belong to this class.

A central observation of our analysis is that

- a "tension" exists between the two observables ϵ_K and BR $(b \to s\gamma)$ in the sense that they have opposite dependence on the composite site Yukawa coupling so that it is *not* possible to simultaneously suppress both these flavor violating effects using this parameter[3].

However, ϵ_K can be suppressed by choosing small composite site QCD coupling. We find that

- $\sim O(5)$ TeV mass scale for the heavy states is allowed simultaneously by ϵ_K and BR $(b \to s\gamma)$ for a size of the composite site QCD gauge coupling corresponding to loop-level matching of the $5D$ QCD coupling (with no tree-level brane kinetic terms) to the $4D$ coupling in the $5D$ model which addresses the Planck-weak hierarchy.

In fact, we argue that,

- once we include color factors in the *estimate* of the loop expansion parameter, a $5D$ QCD coupling larger than the above value might lead to the $5D$ theory no longer being perturbative.

Note that, even with the above smallest value of the $5D$ QCD coupling, the lower limit on mass scale of new particles is different for the two-site model ($\sim O(5)$ TeV) as compared to the $5D$ model with brane-localized Higgs (~ 10 TeV). This is partly due to the fact that, in spite of the two-site model being a deconstruction of the $5D$ model, the detailed features of the two models are different. Secondly, the above bound for the two-site model is from a *combination* of ϵ_K and BR $(b \to s\gamma)$, whereas that for the brane-localized Higgs model is from ϵ_K only.

In fact, we compare in detail our results for the two-site model to those in $5D$ AdS models. In particular, we find that

- the *relations* between the couplings of various particles (at least the ones relevant to ϵ_K) in the two-site model "mimic" those between the corresponding couplings in models with *bulk* Higgs, instead of the case of brane-localized Higgs which has been analyzed in the literature thus far.

---

[2] *Estimates* for $b \to s\gamma$ in the $5D$ AdS model were performed in references [13, 22].

[3] A similar effect was found earlier with regard to the $5D$ Yukawa coupling during an analysis of lepton flavor violation in the $5D$ AdS model [23]

So, our bounds from ϵ_K for the two-site model apply directly to the $5D$ AdS models with bulk Higgs (of a specific profile) for the choice of composite gauge and Yukawa site couplings being same as the corresponding purely KK couplings in the $5D$ model. And, we expect a tension between ϵ_K and $b \to s\gamma$ in the $5D$ AdS model (similar to that in the two-site model). Thus our analysis for the two-site model suggests that a KK scale as low as $\sim O(5)$ TeV might also be allowed in the $5D$ AdS models with bulk Higgs by the *combined* constraints from ϵ_K and BR $(b \to s\gamma)$. On the other hand, we show that

- if, instead of using $b \to s\gamma$ to place an upper bound on the $5D$ Yukawa, we restrict it only by the requirement that two KK modes in the $5D$ EFT are allowed, then a KK mass scale as low as $\sim O(3)$ TeV might be consistent with the constraints from ϵ_K (only) in the $5D$ model with *bulk* Higgs.

The outline of the rest of our paper is as follows. We begin with a review of the relevant features of two-site model, especially the couplings which will be used in our analysis of flavor constraints on this model. Assuming anarchic composite site Yukawa couplings, one typically finds multiple terms (of similar size) in the flavor-violating amplitudes, with $O(1)$ free parameters in the mixing angles and phases so that we need to scan over these parameters. It is then useful to present *analytical* formulae for *one* such generic contribution (with mixing angles set to their "natural" size) in ϵ_K and $b \to s\gamma$. This exercise is presented in sections 3 and 4, providing an *estimate* of the bounds. In section 5, we briefly discuss the bound from $Zb\bar{b}$, which (although not flavor-violating) turns out to be relevant for the analysis of flavor violation. The results of the *numerical* analysis which includes the full amplitudes (summing up all terms) for ϵ_K and $b \to s\gamma$ (and $Zb\bar{b}$) are presented in section 6. The allowed value of $\sim O(5)$ TeV for mass scale of heavy particles in the two-site model mentioned above is based on a combination of the numerical analysis and the analytical estimates. We conclude in section 7. Several appendices deal with further aspects of our analysis. In particular, here we briefly discuss other contributions to ϵ_K and other B-physics observables which provide weaker constraints on the two-site model. We present details of the loop calculation for $b \to s\gamma$ and the exact (numerical) scanning procedure that we used. In a final appendix, we contrast our results for the two-site model with those for the $5D$ AdS model. This comparison is summarized in Table 1.

2 Review of Two-Site Model

2.1 Elementary and Composite Sectors

In this section, we review the basic features of the two-site model (for more details see [30]). The particle content is divided into two sectors: composite and elementary. The elementary sector of the model is equal exactly to that of SM except for the Higgs field. The SM gauge fields ($SU(3) \otimes SU(2)_L \otimes U(1)_Y$) will be denoted in the following way,

$$A_\mu \equiv \{G_\mu, W_\mu, B_\mu\} \tag{1}$$

and fermion $SU(2)_L$ doublets by,

$$\psi_L \equiv \{q_{Li} = (u_{Li}, d_{Li}), l_{Li} = (\nu_{Li}, e_{Li})\} \tag{2}$$

and finally $SU(2)_L$ singlets as,

$$\tilde{\psi}_R \equiv \{u_{Ri}, d_{Ri}, \nu_{Ri}, e_{Ri}\}. \tag{3}$$

The only renormalizable interactions are the gauge interactions.

$$\mathcal{L}^{\text{elementary}} = -\frac{1}{4}F_{\mu\nu}^2 + \bar{\psi}_L i \not{D} \psi_L + \bar{\tilde{\psi}}_R i \not{D} \tilde{\psi}_R. \tag{4}$$

The composite boson sector (containing the SM Higgs and massive spin 1 particles) has $SU(3) \otimes SU(2)_L \otimes SU(2)_R \otimes U(1)_X$ global symmetries, where we need the additional custodial $SU(2)_R$ to suppress new physics contribution to the T parameter [7]. There are fifteen heavy vector mesons (ρ_μ) that belong to adjoint representation of the $SU(3) \otimes SU(2)_L \otimes SU(2)_R \otimes U(1)_X$, and they can be decomposed into two sets: ρ_*, which are in the adjoint representation of the SM gauge group and their orthogonal combinations $\tilde{\rho}$

$$\rho^*_\mu = \{G^*_\mu, W^*_\mu, \mathcal{B}^*_\mu\}, \qquad \tilde{\rho}_\mu = \left\{\tilde{W}^\pm_\mu \equiv \frac{\tilde{W}_1 \mp i\,\tilde{W}_2}{\sqrt{2}}, \tilde{\mathcal{B}}_\mu\right\}. \tag{5}$$

We associate $\mathcal{B}^*, \tilde{\mathcal{B}}$ with the generators $T_{\mathcal{B}^*} = Y_{\text{hypercharge}} = \frac{T^{3R}+\sqrt{2/3}T_X}{\sqrt{5/3}}$ and $T_{\tilde{\mathcal{B}}} = \frac{T^{3R}-\sqrt{2/3}T_X}{\sqrt{5/3}}$, where $T_{\mathcal{B}^*}$ is hypercharge generator in the SO(10) normalization. Higgs field belongs to the composite sector and is a real bidoublet under $SU(2)_L \otimes SU(2)_R$: $(H, \tilde{H})$.

Every SM fermion representation will be accompanied by a heavy composite Dirac fermion, so the composite sector will consist of $SU(2)_L$ doublets :

$$\chi \equiv (Q_i = \{U_i, D_i\}, L_i = \{N_i, E_i\}) \tag{6}$$

and $SU(2)_L$ singlets:

$$\tilde{\chi} = \left(\tilde{U}_i, \tilde{D}_i, \tilde{E}_i, \tilde{N}_i\right) \tag{7}$$

They are all singlets under $SU(2)_R$. The Dirac masses of the composite sector doublets and singlets are $m_*, \tilde{m}_*$, respectively, which we assume to be the same (and generation-independent) for simplicity. $U(1)_X$ charges for fermions are chosen to reproduce the usual SM hypercharges.

The Lagrangian of the composite sector is

$$\mathcal{L}_{\text{composite}} = -\frac{1}{4}\rho_{\mu\nu}^2 + \frac{M_*^2}{2}\rho_\mu^2 + |D_\mu H|^2 - V(H) + \\ +\bar{\chi}(i\not{D} - m_*)\chi + \bar{\tilde{\chi}}(i\not{D} - \tilde{m}_*)\tilde{\chi} - \bar{\chi}(Y_*^u \tilde{H}\tilde{\chi}^u + Y_*^d H\tilde{\chi}^d) + h.c. \tag{8}$$

where M_* is the mass of the composite sector vector boson (again, assumed to be the same for all gauge bosons for simplicity). One can see that Yukawa couplings explicitly break $SU(2)_R$ in composite sector (see Eq. (8)). But this breaking gives a small contribution to the T parameter and is thus technically natural as mentioned in [30].[4]

2.2 Mixing and Diagonalization

The two sectors (composite and elementary) are connected to each other by the mixing terms

$$\mathcal{L}_{\text{mixing}} = -M_*^2 \frac{g_{el}}{g_*} A_\mu \rho_\mu^* + \frac{M_*^2}{2}\left(\frac{g_{el}}{g_*}A_\mu\right)^2 + (\bar{\psi}_L \Delta \chi_R + \bar{\tilde{\psi}}_R \tilde{\Delta}\tilde{\chi}_L + \text{h.c.}). \tag{9}$$

Due to the presence of the gauge boson mixing terms the following combination of the vector bosons will remain massless

$$\frac{g_*}{\sqrt{g_{el}^2 + g_*^2}} A_\mu + \frac{g_{el}}{\sqrt{g_{el}^2 + g_*^2}} \rho_\mu^*. \tag{10}$$

The original elementary and composite states will be re-written using the mass eigenstates as follows

$$\begin{pmatrix} A_\mu \\ \rho_\mu^* \end{pmatrix} \to \begin{pmatrix} \cos\theta & -\sin\theta \\ \sin\theta & \cos\theta \end{pmatrix} \begin{pmatrix} A_\mu \\ \rho_\mu^* \end{pmatrix}, \qquad \tan\theta = \frac{g_{el}}{g_*}, \tag{11}$$

$$\begin{pmatrix} \psi_L \\ \chi_L \end{pmatrix} \to \begin{pmatrix} \cos\varphi_{\psi_L} & -\sin\varphi_{\psi_L} \\ \sin\varphi_{\psi_L} & \cos\varphi_{\psi_L} \end{pmatrix} \begin{pmatrix} \psi_L \\ \chi_L \end{pmatrix}, \qquad \tan\varphi_{\psi_L} = \frac{\Delta}{m_*}, \tag{12}$$

$$\begin{pmatrix} \tilde{\psi}_R \\ \tilde{\chi}_R \end{pmatrix} \to \begin{pmatrix} \cos\varphi_{\tilde{\psi}_R} & -\sin\varphi_{\tilde{\psi}_R} \\ \sin\varphi_{\tilde{\psi}_R} & \cos\varphi_{\tilde{\psi}_R} \end{pmatrix} \begin{pmatrix} \tilde{\psi}_R \\ \tilde{\chi}_R \end{pmatrix}, \qquad \tan\varphi_{\tilde{\psi}_R} = \frac{\tilde{\Delta}}{\tilde{m}_*}. \tag{13}$$

In the new, i.e., mass eigenstate basis, $(A_\mu, \psi_L, \tilde{\psi}_R)$ are the SM fields, which are massless *before* EWSB, and $(\rho_*^\mu, \chi_L, \tilde{\chi}_R)$ are the heavy mass eigenstates (i.e. the heavy partners of SM), again prior to EWSB. To shorten our notations we will denote

$$\theta \equiv \theta_1, \theta_2, \theta_3, \quad \varphi_{\psi_L} \equiv \varphi_{q_{Li}}, \varphi_{l_{Li}}, \quad \varphi_{\tilde{\psi}_R} \equiv \varphi_{u_{Ri}}, \varphi_{d_{Ri}}, \varphi_{\nu_{Ri}}, \varphi_{e_{Ri}} \\ \sin\varphi_{u_R^i} \equiv s_u, \quad \sin\varphi_{d_R^i} \equiv s_d, \quad \sin\varphi_{q_{Li}} \equiv s_q. \tag{14}$$

---

[4] Alternatively, we can add extra composite site fermions so that Yukawa interactions respect $SU(2)_R$. This corresponds to choosing $5D$ fermions in complete multiplets of $SU(2)_R$ in the $5D$ AdS models [7]. We will not pursue this option here.

2.3 Couplings in mass eigenstates before EWSB

Substituting Eq. (11) (12) (13) in Eq. (8), we get the Lagrangian for the Yukawa interaction between quarks and Higgs field in mass eigenstates before EWSB (the same expression will be true for leptons too, one just has to substitute $L, E, N \Longleftrightarrow Q, D, U$)

$$
\begin{aligned}
\mathcal{L}_Y = \quad & \mathcal{L}_Y^{\text{SM-SM}} + \mathcal{L}_Y^{\text{SM-Heavy}} + \mathcal{L}_Y^{\text{Heavy-Heavy}} \\
= \quad & -Y_{*u}\tilde{H} s_q s_u \bar{q}_L u_R - Y_{*d} H s_q s_d \bar{q}_L d_R \\
& -Y_{*u}\tilde{H}\left[c_q s_u \bar{Q}_L u_R + s_q c_u \bar{q}_L \tilde{U}_R\right] - Y_{*d} H \left[c_q s_d \bar{Q}_L d_R + s_q c_d \bar{q}_L \tilde{D}_R\right] \\
& -Y_{*u}\tilde{H}\left[c_q c_u \bar{Q}_L \tilde{U}_R + \bar{Q}_R \tilde{U}_L\right] - Y_{*d} H \left[c_q c_d \bar{Q}_L \tilde{D}_R + \bar{Q}_R \tilde{D}_L\right] + \text{h.c.} \qquad (15)
\end{aligned}
$$

where $c_{q,u,d}$ stands for $\cos(\varphi_{q,u,d})$. We have split the Yukawa interactions into three parts, (SM-SM): interaction between two SM fermions, (SM-Heavy): interaction between SM fermion and heavy fermions, and (Heavy-Heavy): interaction between two heavy fermions.

Similarly interactions between fermions (including SM and heavy) and heavy partners of SM gauge bosons are

$$
\begin{aligned}
& \mathcal{L} = \mathcal{L}^{\text{SM-SM}} + \mathcal{L}^{\text{SM-Heavy}} + \mathcal{L}^{\text{Heavy-Heavy}} \\
& = \rho_\mu^* g \left[\bar{q}_L \gamma_\mu q_L (-c_q^2 t + s_q^2 \frac{1}{t})\right] \\
& + \rho_\mu^* g \left[(\bar{q}_L \gamma_\mu Q_L + \bar{Q}_L \gamma_\mu q_L)(s_q c_q (1 + \frac{1}{t}))\right] \\
& + \rho_\mu^* g \left[\bar{Q}_L \gamma_\mu Q_L (c_q^2 \frac{1}{t} - s_q^2 t)\right] \\
& + \{L \leftrightarrow R\}, \qquad (16)
\end{aligned}
$$

where $t \equiv \tan\theta$, and g is usual SM gauge coupling constant, and it is equal to $g = g_{el}\cos\theta = g_*\sin\theta$. In the same way as we have done for the Yukawa interactions we split total Lagrangian into three parts ((SM-SM), (SM-Heavy), (Heavy-Heavy)) . In the limit when all the SM fermions are made up of mostly elementary sector particles, i.e. $s_q \ll 1$, then the flavor non-universal interaction between SM quarks and heavy gauge bosons will be $\frac{g s_q^2}{\tan\theta} = g_* s_q^2 \cos\theta \approx g_* s_q^2$, and similarly for the right handed quarks.

The interactions between Higgs field, massless vector bosons and their heavy partners are

$$\begin{aligned}
\mathcal{L} = \quad & \mathcal{L}^{\text{SM-SM}} + \mathcal{L}^{\text{SM-Heavy}} + \mathcal{L}^{\text{Heavy-Heavy}} = |D_\mu H|^2 \\
& + \left[H^\dagger i g \cot\theta \rho^*_\mu D_\mu H - i \frac{g_1}{2\sin\theta_1} \left(\frac{1}{\sqrt{2}} \tilde{H}^\dagger \tilde{W}^-_\mu D_\mu H + \frac{1}{\sqrt{2}} H^\dagger \tilde{W}^+_\mu D_\mu \tilde{H} - \sqrt{\frac{3}{5}} H^\dagger \tilde{\mathcal{B}} D_\mu H \right) \right] \\
& + \left[-g_1 g \frac{\cot\theta}{2\sin\theta_1} \left(\frac{1}{\sqrt{2}} \tilde{H}^\dagger \tilde{W}^-_\mu \rho^*_\mu H + \frac{1}{\sqrt{2}} H^\dagger \tilde{W}^+_\mu \rho^*_\mu \tilde{H} - \sqrt{\frac{3}{5}} H^\dagger \tilde{\mathcal{B}} \rho^*_\mu H \right) \right. \\
& \left. + H^\dagger \left((g \cot\theta \rho^*_\mu)^2 + \frac{g_1^2}{\sin^2\theta_1} (\frac{1}{2} \tilde{W}^+_\mu \tilde{W}^-_\mu + \frac{3}{20} \mathcal{B}^2_\mu) \right) H \right] \qquad (17)
\end{aligned}$$

2.4 Flavor Anarchy

We make the assumption that composite site Yukawa couplings are "anarchical", i.e., there is no large hierarchy between elements within each matrix $Y_{*\,u,d}$. However, we need hierarchies in the elementary/composite mixing angles ($s_{q,u,d}$) to reproduce the hierarchical quark masses and CKM mixing angles. Such a choice appears arbitrary from the point of view of the two-site model, i.e., why some couplings are hierarchical and others are not, but this choice will be justified by the correspondence with the 5D model (see Appendix E).

2.5 Including EWSB

Plugging in the Higgs vev in Eq. (15)(17) will lead to new mixings between SM massless fields and their heavy partners which can be classified in the same way as was done in Eq. (15),(16),(17): (SM-SM)- mixing between different generations of the SM massless fermions and the mixing between (W^3, B) SM gauge fields ; (SM-Heavy)- mixing between SM massless fermions and heavy fermions and the mixing between (B, W^3) SM gauge bosons and $(W^3_*, \mathcal{B}_*, \tilde{\mathcal{B}}_*, W_*)$ heavy vector bosons; (Heavy-Heavy)- mixing between the heavy fermions corresponding to the different generations of SM and the mixing between $(W^3_*, \mathcal{B}_*, \tilde{\mathcal{B}}_*, W_*)$ heavy vector bosons. These mixings lead to many new contributions to flavor violating processes, which we will study in detail in later sections.

3 $\Delta F = 2$ processes: ϵ_K

3.1 Formulae for Two-Site Model

We want to find the bound on composite sector scale from CP violation in the $\Delta S = 2$ process, i.e., ϵ_K. The most general effective Hamiltonian for $\Delta S = 2$ processes can be parameterized in the following way [34]

$$
\begin{gathered}
H_{\Delta S=2} = C_1\mathcal{O}_1 + C_2\mathcal{O}_2 + C_3\mathcal{O}_3 + C_4\mathcal{O}_4 + C_5\mathcal{O}_5 \text{ with} \\
\mathcal{O}_1 = \bar{d}^\alpha_L \gamma_\mu s^\alpha_L \bar{d}^\beta_L \gamma_\mu s^\beta_L, \quad \mathcal{O}_2 = \bar{d}^\alpha_R s^\alpha_L \bar{d}^\beta_R s^\beta_L \\
\mathcal{O}_3 = \bar{d}^\alpha_R s^\beta_L \bar{d}^\beta_R s^\alpha_L, \quad \mathcal{O}_4 = \bar{d}^\alpha_R s^\alpha_L \bar{d}^\beta_L s^\beta_R, \quad \mathcal{O}_5 = \bar{d}^\alpha_R s^\beta_L \bar{d}^\beta_L s^\alpha_R,
\end{gathered} \tag{18}
$$

where α, β are color indices. There are also $\mathcal{O}'_{\infty,\in}$ operators with L replaced by R. The dominant contributions to these Wilson coefficients in the two-site model come from tree-level exchange of heavy gauge bosons – for example gluon (see Fig. 1) – with flavor violating couplings. These flavor violating couplings arise mainly from the mixings between SM fermions induced after EWSB (see section 2.5) which we now focus on – the other two types of mixings (SM-Heavy, Heavy-Heavy) have sub-leading effects for ϵ_K and so will be neglected for the analysis in this section.

The point is that the couplings between heavy gluon and SM quarks are diagonal but non-universal in the gauge eigenstate basis for quarks, i.e., before EWSB, in $\mathcal{L}^{\text{SM-SM}}$ term of Eq. (16). After EWSB, one has to use unitary transformations: $(D_L,\ D_R)$ and $(U_L,\ U_R)$ to go to mass eigenstate basis for down and up-type quarks respectively (just like in the SM). These rotations thus lead to off-diagonal couplings between SM quarks (in mass eigenstate basis) and heavy gluon. From the analysis of the $5D$ models [16, 17, 14, 15], it is well-known that the dominant contribution comes from the heavy/KK gluon exchange between left-handed and right-handed down-type quark currents, i.e., $(V-A)\times(V+A)$-type operators. Therefore, we focus here on heavy gluon exchange of the above type. It is straightforward to show that such exchange gives (upon Fierzing)

$$
\begin{aligned}
C_4\left(M_*\right) &= -3C_5\left(M_*\right) \\
&= \frac{\left(g_{s*}\right)^2}{M_*^2}\left[\left(s_{q2}\right)^2\left(D_L\right)_{12} + \left(s_{q3}\right)^2\left(D_L\right)_{13}\left(D_L\right)_{23}\right] \times \\
&\quad \left[\left(s_{d2}\right)^2\left(D_R\right)_{12} + \left(s_{d3}\right)^2\left(D_R\right)_{13}\left(D_R\right)_{23}\right]^*
\end{aligned} \tag{19}
$$

where g_{s*} is composite QCD coupling. Each $\left[...\right]$ in this formula includes two terms, i.e., one from the "direct" $1-2$ mixing (present even with two generations) and another from the $(1-3)\times(2-3)$ mixing (i.e., via 3rd generation) for the left and right-handed flavor-violating couplings.

Assumption of anarchic Yukawa couplings Y_* in the original Lagrangian of Eq. (15) implies that mixing angles in SM Yukawa couplings are given by ratios of elementary-composite mixings[13], for example,

$$
\left(D_{L,R}\right)_{ij} \sim \frac{(s_{q,d})_i}{(s_{q,d})_j} \text{ for } i<j \tag{20}
$$

So, the two terms (inside each of the brackets $\left[...\right]$) in Eq. (19) (for each of left and right-handed sectors) are of same size, but uncorrelated.

On the other hand from the $\mathcal{L}_Y^{\text{SM-SM}}$ term of Eq. (15) we have

$$m_d \sim Y_*^d s_{q1} s_{d1} v/\sqrt{2} \qquad (21)$$
$$m_s \sim Y_*^d s_{q2} s_{d2} v/\sqrt{2},$$

so we can estimate the size of the mixing angles s_{qi}, s_{di}.

Now we can estimate new physics contribution to $C_{4,\,5}$ using the following assumptions: (i) considering one term in each of the brackets $\Big[...\Big]$ of Eq. (19) at a time, (ii) mixing angles set to "natural" size (i.e., with "=" in Eq.(20) above), and (iii) quark masses given by natural size of the parameters (i.e., with "=" in Eq.(21) above). Plugging Eq. (20) and (21) into Eq. (19) leads to the estimate, up to an $O(1)$ complex factor:

$$C_{4\ \text{estimate}}^{2-\text{site}} = \frac{g_{s*}^2}{(Y_*^d)^2}\frac{2m_s m_d}{v^2}\frac{1}{M_*^2} \qquad (22)$$

with $v = 246$ GeV, where subscript "estimate" stands for the above three assumptions. To repeat, the assumption of anarchy tells us that the four terms in Eq. (19) are of the same size as Eq. (22) and have *un*correlated phases. Therefore, our estimate using one term gives us the correct result up to $O(1)$ factor.

3.2 Experimental limit

The model independent bound from ϵ_K is strongest on the Wilson coefficient C_4 due to (i) enhancement (as compared to for the other Wilson coefficients) from RG scaling from the new physics scale to the hadronic scale and (ii) from chiral enhancement of matrix element (see reference [35]).[5] This bound on C_4 is :

$$\text{Im}\, C_4 \lesssim \frac{1}{(\Lambda_F)^2}, \qquad \Lambda_F = 1.6 \times 10^5\,\text{TeV}. \qquad (23)$$

where the coefficient is renormalized at the ~ 3 TeV scale [14]. Note that the bound on Im C_4 is only mildly (logarithmically) sensitive to the renormalization scale and hence it remains almost the same as the above number (which is again for a scale of ~ 3 TeV) for heavy mass scales of up to ~ 10 TeV that we will consider in this paper. Using Eqs. (22) and (23), and assuming order one phase, we get

$$M_* \gtrsim \frac{11 g_{s*}}{Y_*^d}\ \text{TeV} \qquad (24)$$

We can see the bound on the composite mass scale *decreases* as Y_*^d increases.

---

[5] The effect of $C_5\,(M_*)$ in the two-site model is sub-leading because firstly the model-independent bound is weaker relative to C_4 (see reference [35]) and secondly in this model $C_5\,(M_*)$ is suppressed by a color factor relative to C_4 (see Eq. 19).

4 Radiative processes: $b \to s\gamma$

The rare decay $B \to X_s\gamma$ gives very powerful constraints on new physics. We follow the standard notation and define the effective Hamiltonian for $b \to s\gamma$ [34]:

$$\mathcal{H}_{eff}(b \to s\gamma) = -\frac{G_F}{\sqrt{2}} V_{ts}^* V_{tb} [C_7(\mu_b) Q_7 + C_7'(\mu_b) Q_7' + \ldots] \tag{25}$$

where $Q_7 = e\ m_b / \left(8\pi^2\right) \bar{b}\sigma^{\mu\nu} F_{\mu\nu}(1-\gamma_5)s$ and $Q_7' = m_b\ e\left(8\pi^2\right) \bar{b}\sigma^{\mu\nu} F_{\mu\nu}(1+\gamma_5)s$. Here we have neglected other operators that only enter through renormalization of C_7 and C_7'. In SM, the Wilson coefficient $C_7(\mu_w)$ evaluated at weak scale is[34]

$$C_7^{SM}(\mu_w) = -\frac{1}{2}\left[-\frac{(8x_t^3 + 5x_t^2 - 7x_t)}{12(1-x_t)^3} + \frac{x_t^2(2-3x_t)}{2(1-x_t)^4}\ln(x_t)\right]; \qquad C_7'^{\,SM}(\mu_w) = \frac{m_s}{m_b} C_7^{SM}(\mu_w) \tag{26}$$

with $x_t = m_t^2/M_w^2$. The Wilson coefficient $C_7'(\mu_w)$ can be neglected in SM due to a suppression by m_s/m_b. The leading order QCD correction gives us [34]

$$\begin{aligned} C_7(\mu_b) &= 0.695 C_7(\mu_w) + 0.085 C_8(\mu_w) - 0.158 C_2(\mu_w) \\ &= 0.695(-0.193) + 0.085(-0.096) - 0.158 = -0.300 \end{aligned} \tag{27}$$

where C_2 and C_8 are Wilson coefficients for operators $Q_2 \equiv (\bar{c}b)_{V-A}(\bar{s}c)_{V-A}$ and $Q_{8G} \equiv m_b\ g/\left(8\pi^2\right) \bar{b}_\alpha \sigma^{\mu\nu}(1-\gamma_5) T^a_{\alpha\beta} s_\beta G^a_{\mu\nu}$. The latest higher order calculations for BR($b \longrightarrow s\gamma$) are given in [36] but the above order results suffice for our purposes.

4.1 Estimate in two-site model

In two-site model, the largest new physics contribution to $\Gamma(b \to s\gamma)$ comes from diagrams with heavy states in the loop because of their larger coupling constants. First, we consider diagrams with heavy gluons and fermions (see Fig. 2). We can get an idea of the flavor structure of this diagram by treating the EWSB-induced fermion mass terms of Eq. (15) as being small compared to the masses of the heavy partners of SM fermions (henceforth called by the mass insertion approximation). From $\mathcal{L}^{\text{SM-Heavy}}$ term of Eq. (16), we see that mass insertion approximation gives us a new contribution to Wilson coefficients of operators $\bar{d}_j \sigma^{\mu\nu} F_{\mu\nu}(1-\gamma_5) d_i$ (with quarks in gauge basis before EWSB)

$$C^G_{7\,ij} \propto s_{q_i} g_{s*}^2 Y^d_{*ij} s_{d_j} \tag{28}$$

Notice that C^G_{7ij} has the same flavor structure as quark mass matrix $m_{d\,ij} \approx Y^d_{*\,ij} s_{q_i} s_{d_j}$. Therefore, after unitary rotation into the mass eigenstates after EWSB, C^G_{7ij} will be approximately diagonal in flavor space, and contribution from heavy gluon and heavy fermion exchange to $\Gamma(b \to s\gamma)$ is suppressed. (see reference [13] for a similar discussion in warped extra dimension, where KK gluons and KK fermions correspond to heavy gluons and fermions here.)

Next, we consider diagrams with heavy fermions and Higgs in the loop (including physical Higgs and longitudinal W/Z bosons). Similar to the previous analysis, we can get the flavor structure of these diagrams from mass insertion approximation. For the purpose of estimating flavor structure, we consider only neutral Higgs diagram (see Fig. 4). From the Yukawa couplings between SM fermion, heavy fermion and Higgs ($\mathcal{L}^{\text{SM-Heavy}}$ term of Eq. 15), we find that

$$C^H_{7\,ij} \propto s_{q_i} Y^d_{*ik} Y^d_{*kl} Y^d_{*lj} s_{d_j} \tag{29}$$

It is obvious that $C^H_{7\,ij}$ is not aligned with $m_{d\,ij}$, assuming no particular structure in the Y_* (i.e., anarchy). Thus these diagrams will give the leading new contribution to C_7 and C_7', and we will focus on these diagrams (see reference [13] for a similar discussion in warped extra dimension).

Because of the near degeneracy of heavy fermion masses, we can*not* use mass insertion approximation to *calculate* the loop diagrams. Instead, we need to diagonalize the 9×9 mass matrix (once we include EWSB-induced mass terms, i.e., coming from Yukawa couplings in Eq. (15)) for all down type quarks in order to determine the mass eigenstates and their couplings. Since it is difficult to obtain an exact analytical formulae for this effect, the analysis is performed numerically in Section 6. However, it is insightful to obtain an approximate analytical formulae for $b \rightarrow s\gamma$ as follows. First, we calculate the dipole operator for the case of *one* generation quark together with its heavy partners (say, as in the calculation of $(g-2)_\mu$)) with*out* using the mass insertion approximation and then we simply multiply it by factors from generational mixing effects in order to obtain the amplitude for $b \rightarrow s\gamma$.

In more detail, we diagonalize the 3×3 mass matrix (including the EWSB-induced mass terms) for one generation quarks analytically to first order in $x \equiv Y^{u,d}_* v / \left(m_* \sqrt{2}\right)$ in Appendix B: the results for dipole moment operator of one generation with charged and neutral Higgs in the loop are shown in Eqs. (67) and (71). In order to *estimate* the effect of mixing between different generations, we again use mass insertion approximation (see Fig. 4). For example, the operator $\bar{b}_L \sigma^{\mu\nu} F_{\mu\nu} s_R$ can be generated via the mass insertions/Yukawa couplings (as in Eq. 29, but dropping the flavor indices on Y_{d*} for simplicity)

$$Y_{d*} s_{q3} Y_{d*} v Y_{d*} s_{d2} \tag{30}$$

Based on our assumption of anarchy and the formulae for Yukawa couplings and mixing angles (Eq. (15) (20)), we know that

$$Y_{d*} v s_{q3} s_{d2} = Y_{d*} v s_{q3} s_{d3} \frac{s_{d2}}{s_{d3}} \sim m_b (D_R)_{23} \tag{31}$$

and

$$\frac{m_s}{m_b} \;\sim\; (D_L)_{23} \, (D_R)_{23} \tag{32}$$

In addition, since left-handed down and up-type quarks have the same elementary-composite mixing, we get (again assuming anarchy of Y_{d*})

$$\begin{aligned} (D_L)_{23} &\sim (U_L)_{23} \\ &\sim V_{ts} \text{ or } V_{cb} \end{aligned} \tag{33}$$

where in the second line we have used that $V_{CKM} = U_L^\dagger D_L$. Combining Eq (30) through (33), we can find that generational mixing gives a factor $\sim \frac{m_s}{m_b V_{ts}}$. Similarly, for the operator $\bar{b}_R \sigma^{\mu\nu} F_{\mu\nu} s_L$ we have (as in Eq. 29)

$$Y_{d*} s_{d3} Y_{d*} v Y_{d*} s_{q2} \sim (Y_{d*})^2 m_b (D_L)_{23} \sim (Y_{d*})^2 m_b V_{ts} \tag{34}$$

i.e., generational mixing gives a factor $\sim V_{ts}$. Note that for neutral Higgs diagram the amplitude is proportional to Y_{d*}^3. The flavor structure for *charged* Higgs (would-be Goldstone) diagram is similar, expect that there are two types of contributions (schematically $\propto Y_{d*}^3$ and $Y_{u*}^2 Y_{d*}$). For simplicity, we set $Y_{u*} = Y_{d*} \equiv Y_*$ in our estimation.

Then, multiplying the one generation results for dipole operator in Eqs. (67) and (71) by the above generational mixing factors, we get the following effective Hamiltonians:

$$\mathcal{H}^{eff}_{\text{charged Higgs}} \approx \frac{5}{12} (Y_*)^2 m_b \frac{ie}{16\pi^2} \frac{(2\epsilon \cdot p)}{(m_*)^2} [V_{ts} \bar{b}(1-\gamma_5)s + \frac{m_s}{m_b V_{ts}} \bar{b}(1+\gamma_5)s] \tag{35}$$

$$\mathcal{H}^{eff}_{\text{neutral Higgs}} \approx -\frac{1}{4} (Y_*)^2 m_b \frac{ie}{16\pi^2} \frac{(2\epsilon \cdot p)}{(m_*)^2} [V_{ts} \bar{b}(1-\gamma_5)s + \frac{m_s}{m_b V_{ts}} \bar{b}(1+\gamma_5)s] \tag{36}$$

We present the results for both charged Higgs and neutral Higgs contribution since they generally have different phase and cannot be simply added together. Since their sizes are of the same order, we will *focus just on charged Higgs contribution in the analytical estimates.* Then, the new physics contribution to the Wilson coefficients are[6]

$$C^{2-\text{site}}_{7\,\text{estimate}}(m_*) = -\frac{5}{48} \frac{(Y_*)^2}{(m_*)^2} \frac{\sqrt{2}}{G_F}; \qquad C'^{2-\text{site}}_{7\,\text{estimate}}(m_*) = -\frac{5}{48} \frac{(Y_*)^2}{(m_*)^2} \frac{\sqrt{2}}{G_F} \frac{m_s}{m_b \lambda^4} \tag{37}$$

where we used $V_{ts} \sim \lambda^2$ ($\lambda \approx 0.22$). As explained earlier, (based on assumption of anarchy) in the exact result for $b \to s\gamma$ there will be several terms of the above order but with uncorrelated phases. Thus Eq. (37) is only an *estimate* for $b \to s\gamma$, i.e., the natural size of *one* term that contribute to the new physics effective Hamiltonian. We expect the final result of the coherent sum of such terms to be of the same order as this one-term estimates. From these estimates we can conclude that $C_7^{\prime 2-\mathrm{site}}(m_*)$ is bigger than $C_7^{2-\mathrm{site}}(m_*)$ by a factor of $m_s/\left(m_b V_{ts}^2\right) \sim 8$, which is different than the case in SM (where $C_7^\prime \approx C_7\ m_s/m_b$).

---

[6] Note that such a size for these Wilson coefficients can be *estimated*, i.e., derived up to $O(1)$ factors, using *purely* mass insertion approximation. As explained above, here instead we have *calculated* the $O(1)$ factor from loop diagram (with*out* using mass insertion approximation), although we still used mass insertion approximation to estimate the generational mixing factors.

As mentioned earlier, in Section 6, we will apply the exact diagonalization of the 9×9 mass matrix for three generations to the results from general loop calculation of $b \to s\gamma$ in Appendix A to obtain $C_7^{2-\mathrm{site}}$ and $C_7^{\prime 2-\mathrm{site}}$ numerically.

4.2 Experimental limit

The leading order QCD corrections will suppress the new physics contribution to the Wilson coefficients

$$C_7^{2-\mathrm{site}}(\mu_w) = \left[\frac{\alpha_s(m_*)}{\alpha_s(m_t)}\right]^{16/21} \left[\frac{\alpha_s(m_t)}{\alpha_s(\mu_w)}\right]^{16/23} C_7^{2-\mathrm{site}}(m_*) \approx 0.73\ C_7^{2-\mathrm{site}}(m_*) \tag{38}$$

We add it to $C_7^{\mathrm{SM}}(\mu_w)$ in Eq. (26) and then use this sum, i.e., $C_7^{\mathrm{total}}(\mu_w) = C_7^{\mathrm{SM}}(\mu_w) + C_7^{2-\mathrm{site}}(\mu_w)$ in Eq. (27) to obtain $C_7(\mu_b)$. Whereas, the SM contribution to $C_7^\prime$ is negligible compared to that in the two-site model so that we have

$$\begin{aligned} C_7^{\prime\mathrm{total}}(\mu_b) &\approx C_7^{\prime 2-\mathrm{site}}(\mu_b) \\ &= \left[\frac{\alpha_s(m_*)}{\alpha_s(m_t)}\right]^{16/21} \left[\frac{\alpha_s(m_t)}{\alpha_s(\mu_b)}\right]^{16/23} C_7^{\prime 2-\mathrm{site}}(m_*) \\ &\approx 0.48\ C_7^{\prime 2-\mathrm{site}}(m_*) \end{aligned} \tag{39}$$

The contributions from $C_7(\mu_b)$ and $C_7^\prime(\mu_b)$ sum incoherently (without interference) in the total (i.e., SM and new physics) decay width $\Gamma^{\mathrm{total}}(b \to s\gamma)$:

$$\Gamma^{\mathrm{total}}(b \to s\gamma) \propto |C_7(\mu_b)|^2 + |C_7^\prime(\mu_b)|^2 \tag{40}$$

For convenience, we define $\delta_7 \equiv C_7^{2-\mathrm{site}}(m_*)/C_7^{SM}(\mu_w)$ and $\delta_7^\prime \equiv C_7^{\prime\, 2-\mathrm{site}}(m_*)/C_7^{SM}(\mu_w)$. Adding these new contributions, we have

$$\frac{\Gamma^{\mathrm{total}}(b \to s\gamma)}{\Gamma^{SM}(b \to s\gamma)} \approx 1 + 0.68 Re(\delta_7) + 0.11|\delta_7^\prime|^2 \tag{41}$$

The experimental average value for the branching ratio is $BR(b \to s\gamma) = (352 \pm 23 \pm 9) \times 10^{-6}$[37]. The theoretical calculation gives $BR(b \to s\gamma) = (315 \pm 23) \times 10^{-6}$[38]. Adding the 2σ uncertainties by quadrature we find that a 20% deviation from SM prediction is allowed. If we consider the two contributions separately, we will get the bound $|\delta_7^\prime| \lesssim 1.4$ and $\mathrm{Re}(\delta_7) \lesssim 0.3$. Using Eqs. (37) and (26), the first condition gives

$$m_* \gtrsim (0.63) Y_*\ \mathrm{TeV} \tag{42}$$

and the second condition gives us a weaker bound. From this rough estimate, we can see the bound on composite mass scale *increases* with composite Yukawa coupling.

4.3 Tension and lowest heavy SM partner mass scale scenario

We see that the bounds on M_* and m_* from ϵ_K and BR$(b \to s\gamma)$ have opposite dependence on Y_*. Thus we cannot use this parameter to decouple flavor-violation. *For simplicity, we set* $M_* = m_*$ *henceforth.* Then the lowest allowed value for M_* that satisfies both bounds Eqs.(24) and (42) is

$$\begin{aligned} M_* &\gtrsim 2.6\sqrt{g_{s*}}\ \text{TeV} \quad \text{for} \quad Y_* \sim 4.2\sqrt{g_{s*}} \\ &\sim 4.5\ \text{TeV for } g_{s*} \sim 3 \\ &\sim 6.4\ \text{TeV for } g_{s*} \sim 6 \end{aligned} \tag{43}$$

where in last two lines, we have set $g_{s*} \sim 3, 6$ which is motivated by the $5D$ AdS model, although the latter value might not be allowed by $5D$ perturbativity (see Appendix E.1.1). We can check that with the values of Y_* in Eq. (43), the loop expansion parameter $Y_*^2 / \left(16\pi^2\right)$ is less than one, and the two-site model is thus perturbative (but barely so in the case of $Y_* \sim 10$ for $g_{s*} \sim 6$): see Appendix E.4 about perturbativity bound on KK Yukawa couplings in the $5D$ AdS model.

We reiterate that the bounds in Eq. (43) are only *estimates* in the sense that they are based on *one* among multiple, *uncorrelated* terms in the amplitudes for both ϵ_K and $b \to s\gamma$. Also, note that the contributions to $b \to s\gamma$ in the two-site model, being at the loop-level (as opposed to the tree-level contributions to ϵ_K), can be quite sensitive to the composite sector content – for example, as mentioned in section 2.1, we could add $SU(2)_R$ partners for the composite site u_R and d_R (as in $5D$ models) which can easily modify the new physics amplitude for $b \to s\gamma$ by $\sim O(1)$ factors due to their appearance in the loops. In this sense, the constraints from $b \to s\gamma$ presented for this model should especially be considered as a ballpark guide to the viable parameter space of this framework: the main motivation for using $b \to s\gamma$ in our analysis is to put an upper bound on the composite site Yukawa coupling.

As discussed in references [13, 22] for the $5D$ model, the Higgs-heavy fermion loop contributions to electric dipole moments (EDMs) of SM fermions also increase with the size of the composite Yukawa coupling (just like $b \to s\gamma$). Thus, EDMs can also be used to put an upper bound on the size of this coupling (for a given heavy mass scale). However, EDMs depend on a different (flavor-*preserving*) combination of phases than the flavor-violating observables ϵ_K and $b \to s\gamma$ and so we will leave a study of these constraints for the future. Note that $5D$ flavor symmetries can suppress EDM's as well as the flavor violating effects.

5 Correction to $Zb\bar{b}$ coupling

There is another important constraint coming from non-universal correction to $Zb_L\bar{b}_L$ coupling which arises from mixing between SM and heavy states after EWSB (see [30])

$$\frac{\delta g_{Z\bar{b}b}}{g_{Z\bar{b}b}} \approx \sum_{i=1}^{3} \left(\frac{Y_{*di3}}{Y_{*u33}}\right)^2 \left(\frac{m_t}{M_* s_{u3}}\right)^2 + \frac{1}{2}\left(\frac{m_t}{M_* s_{u3}}\right)^2 \left(\frac{g_{*2}}{Y_{*U33}}\right)^2 \tag{44}$$

Experimentally, it is measured to have less than 0.25% deviation from its SM value. If we assume that all composite Yukawa couplings are of the same order, then we can get a bound on M_* from the first term alone:

$$M_* \gtrsim 4.7 \quad \text{TeV} \tag{45}$$

This bound is similar to what we found from ϵ_K and $b \to s\gamma$. However, if we allow a little hierarchy between the Yukawa couplings, e.g., $Y_{*d} > Y_{*u}$, then the bound on M_* will be enhanced. We mention that $Z\bar{b}_L b_L$ coupling can be protected by another custodial symmetry[10]. But we will not use this idea here.

6 Numerical Analysis

In previous sections we presented semi-analytical *estimates* for the new physics contributions to the ϵ_K and $b \to s\gamma$ processes, but to get the precise values one has to perform a numerical scan over the parameter space. The scan procedure is discussed in detail in Appendix C. Here we summarize some important features and results of our scan. We require that our composite Yukawa coupling matrices are anarchical, i.e. all entries of the same order, with the results presented here corresponding to the variation of the Yukawa couplings by a factor of three, and we varied the elementary/composite mixings also by a factor of three. First, we generate the points in parameter space with $Y_{u*}, Y_{d*}, s_Q, s_u, s_d$ such that the SM quark masses and CKM mixing angles are reproduced. Then we calculated $|\frac{\Gamma^{\text{total}}(b\to s\gamma)}{\Gamma^{\text{SM}}(b\to s\gamma)} - 1|/(20\%)$, $|\delta g_{Z\bar{b}b}/g_{Z\bar{b}b}|$ and $\text{Im}\, C_{4K}\Lambda_F^2$ (with $\Lambda_F = 1.6 \times 10^5$ TeV) for different values of M_* and $Y_*^{u,d}$.

In Fig. 5, we show the plots of $|\frac{\Gamma^{\text{total}(b\to s\gamma)}}{\Gamma^{SM}(b\to s\gamma)} - 1|/(20\%)$ and $\text{Im}\, C_{4K}\Lambda_F^2$ for $M_* = 5$ TeV and different values of $Y_*^{u,d}$ (defined here as the geometric *average* value for $Y_{*ij}^{u,d}$). We focus on the case with $g_{s*} = 3$. Points to the left and below the solid lines satisfy both bounds from BR $(b \to s\gamma)$ and ϵ_K. We begin with the cases with no hierarchy between the up and down-type quark composite site Yukawa coupling, i.e., $Y_*^d = Y_*^u$. In the top left plot, we choose this value to be $\in (3, 4)$. We see that a small fraction of points satisfy the bounds from ϵ_K and BR $(b \to s\gamma)$. Next we increase the common value for Y_*^d and Y_*^u to $(6, 7)$ (top right plot). We expect that the larger Yukawa coupling will enhance the contribution to $\Gamma(b \to s\gamma)$ and suppress the contribution to $\text{Im}\, C_{4K}$, which is clearly shown in the plots and illustrates the tension discussed in section 4.3. In the end, there are fewer points satisfying both bounds with these larger Yukawa couplings.

Finally, we consider a mild hierarchy between the Yukawa couplings: $Y_*^u \in (1, 2)$ and $Y_*^d \in (5, 6)$

(bottom plot). We find that more points satisfy both bounds than in the previous two cases. This is expected since small Y_*^u suppresses one of the contributions to $\Gamma(b \to s\gamma)$[7] while larger Y_*^d suppresses contribution to $\operatorname{Im} C_{4K}$. However, the bound from non-universal $Z\bar{b}_L b_L$ coupling correction is more constrained in this case due to the $(\frac{Y_*^{di3}}{Y_*^{u33}})^2$ enhancement in $\delta g_{Z\bar{b}_L b_L}$ (see Eq. (44)) so that we have to study the consequence of this bound. In Fig. 6, we present the result from the scan for $\operatorname{Im} C_{4K}$ and $\delta g_{Z\bar{b}_L b_L}$. We can see that when $Y_*^d = 5 \sim 6$ and $Y_*^u = 1 \sim 2$ (right plot) the $\delta g_{Z\bar{b}_L b_L}$ bound eliminates a majority of the points. However, for $Y_*^u = Y_*^d \in (3, 4)$ (left plot), the bound on $\delta g_{Z\bar{b}_L b_L}$ is easily satisfied, as expected from our analysis in Section 5.

We show the same scatter plots for $M_* = 10\,\text{TeV}$ (Fig. 7, 8) and $M_* = 3\,\text{TeV}$ (Fig. 9, 10). As it is clearly shown in the plots, all bounds can be easily satisfied for $M_* = 10\,\text{TeV}$, while almost no point satisfy all bounds for $M_* = 3\,\text{TeV}$. Note that, with our choices of Y_*, higher-order loop diagrams with these couplings will give us corrections to all our observables of $\sim Y_*^2/\left(16\pi^2\right) \sim O\left(1/\text{a few}\right) - 1/10$, which is the main source of error in our analysis[8].

Now we consider the case with a larger composite site gluon coupling, i.e., $g_{s*} = 6$. The contribution in the two-site model to $\Gamma(b \to s\gamma)$ is the same as in the case $g_{s*} = 3$ while $\operatorname{Im} C_{4K}$ increases by a factor of 4. Thus, rather than showing separate plots for $g_{s*} = 6$, we can present the *bounds* for this case on the same plots as for $g_{s*} = 3$ by just moving the line from the $\operatorname{Im} C_{4K}$ bound downward by factor of 4. So all the points satisfying both constraints for $g_{s*} = 6$ are below the *dashed* line and to the left of the solid line in the same plots. As expected, for $g_{s*} = 6$, few (a sizable fraction of) points satisfy the bounds for $M_* = 5(10)$ TeV.

Combining the results of the numerical analysis shown in the plots with our earlier estimate in Eqs. (43) and (45) of ~ 4.5 TeV as the lowest heavy SM partner mass scale allowed, we then conclude M_* as low as $\sim O(5)$ TeV with $g_* \sim 3$ can satisfy all the constraints we considered.

7 Conclusions

The warped extra dimensional framework with bulk SM is very well-motivated scenario for beyond the SM since it can address many of the puzzles of nature. The two-site model provides a economical description of this framework by effectively restricting to the SM fields and their first KK excitations. In this paper, we studied constraints on this model from flavor violation in the quark sector, in particular, we showed that ϵ_K and BR $(b \to s\gamma)$ provide the strongest constraints. Moreover, these two observables have opposite dependences on the composite site Yukawa couplings so that this parameter cannot be used to ameliorate the flavor constraints.

---

[7] There is also a contribution $\propto Y_d$ only as discussed in section 4.1.

[8] Of course, we are also incurring an error of similar size due to neglect of higher KK modes in the two-site approach for analyzing the $5D$ model

Assuming anarchic composite site Yukawa couplings and based on both numerical and analytical calculations, we showed that $\sim O(5)$ TeV mass scale for the heavy states can be consistent with both the observables for a size of composite site QCD coupling which is consistent with the $5D$ AdS model solving the Planck-weak hierarchy problem, where the $5D$ QCD coupling is matched to the $4D$ coupling at the loop-level and with negligible brane kinetic terms. We argue that a larger $5D$ coupling might be constrained by the requirement of $5D$ perturbativity.

Moreover, we showed that couplings in the the two-site model are similar to those in the $5D$ models with *bulk* Higgs (but still leaning towards the TeV brane) rather than to the brane-localized Higgs case. Thus our results suggest $\sim O(5)$ TeV KK mass scale might be consistent with quark sector flavor violation even for $5D$ AdS models with bulk Higgs.

With $O(5)$ TeV mass scale, signals at the LHC (including its luminosity upgrade, the SLHC) from direct production of the heavy states are extremely suppressed, in particular, only the heavy gluon might be (barely) accessible [39]. However, with very mild tuning (i.e., deviation from anarchy in the composite site Yukawa couplings), it is clear that $\sim O(3)$ TeV KK scale might be allowed, enhancing the direct LHC signals and making even the EW heavy states possibly accessible at the LHC [40].

Finally, we comment on future signals and constraints from flavor violation. Obviously, the two-site model with $O(5)$ TeV mass scale for the heavy particles is on the edge of ϵ_K and BR $(b \to s\gamma)$ so that reduction of theoretical errors in these observables will provide even stronger constraints on this framework. More broadly speaking, given $\sim O(5)$ TeV scale for the new particles, their contributions to amplitudes for $\Delta F = 2$ and $\Delta F = 1$ processes are typically at the level of $\sim O(10\%)$ of the SM. Such a modest size might be relevant for the hints (i.e., $2 - 3\sigma$ discrepancies in the SM unitarity triangle fit) of beyond-SM effects in B/K physics which are precisely at this level: see references [41] for a general analysis and reference [15] for some discussion in the context of warped extra dimension.

In fact, this size of new amplitudes in the warped framework can still lead to striking deviations from SM, in spite of the (rough) consistency of the SM predictions with the current flavor data. For example, CP violation in B_s mixing is expected to be $\sim O(10\%)$ in this scenario, larger than the SM expectation of a few % (and there might be some hint for such an effect in the data [42]). This prediction can be thoroughly tested at the LHC-b.

An even more dramatic example is that a slightly larger amplitude in $b \to s\gamma$, namely, $\sim O(0.5)$ of SM with *opposite* chirality to that in the SM is still allowed since such a contribution does not interfere with the SM amplitude *in the decay width or BR*, giving an effect in BR $\sim O(20\%)$ which is on the edge of the current constraints. We discussed that in the two-site model, the dominant effect in $b \to s\gamma$ is precisely of such a size in the opposite-to-SM chirality amplitude. The point is that such an effect gives $\sim O(0.5)$ time-dependent mixing-induced CP asymmetry from the interference with the SM amplitude, in sharp contrast to the SM prediction of this CP asymmetry: $m_s/m_b \sim$ a few % (as already pointed out in [22, 13] for the $5D$ models). The current 2σ error on this CP asymmetry is $\sim O(0.5)$ so that there is no strong constraint at present from this observable. However, if in the future, this CP asymmetry can be probed at the SM level or even $\sim O(0.1)$, then we might obtain a striking signal for this model (or an even stronger constraint than $\sim O(5)$ TeV on the mass of new particles). We leave this analysis for a future study.

Acknowledgments

KA was supported in part by NSF grant No. PHY-0652363 and would like to thank Csaba Csaki, Adam Falkowski, Tony Gherghetta, Seung Lee, Takemichi Okui, Michele Papucci, Gilad Perez, Raman Sundrum, Tomer Volansky and Andreas Weiler for discussions and the Aspen Center for Physics for hospitality during part of this work. The authors also thank Csaba Csaki, Adam Falkowski, Gilad Perez and Andreas Weiler for comments on the manuscript.

A Model Independent Loop Calculation

We work in *non*-unitary gauge for the electroweak gauge sector of the SM, where we must include the would-be Goldstone bosons in the loop. The model-*independent* interaction between a *charged* Higgs, SM down-type quarks (d) and an up-type heavy quark (U) can be parametrized as follows:

$$\mathcal{L} \supset \bar{U}[\alpha_{1i}(1+\gamma_5) + \alpha_{2i}(1-\gamma_5)]d_i \; H^- + h.c. \tag{46}$$

where *all quarks are in mass eigenstate basis (including effects of EWSB).* We focus on the dominant contributions to the dipole moment operator for $b \to s\gamma$ generated by these interactions – the relevant diagrams contain the charged Higgs and heavy fermion in the loop with the SM fermions as external legs (see Fig. 3A and B). We will then apply the results obtained in this section for the *specific* case of the two-site model and calculate the effective dipole operator for *one* generation in Appendix B and $b \to s\gamma$ in appendix B.1.

For the first diagram (see Fig. 3A), with photon line attached to the heavy fermion, we get the effective operator[9]

$$\mathcal{H}_1^{\mathrm{e}ff} = \frac{ieQ_U}{8\pi^2}\frac{(2\epsilon \cdot p)}{M_w^2}\left\{A_1 \bar{s}(1+\gamma_5)b + B_1 \bar{s}(1-\gamma_5)b\right\} \tag{47}$$

---

[9] We used Feynman gauge in this calculation. Since we are considering only the dominant diagrams here, the result will be different by $O(\frac{M_w^2}{M_*^2})$ if we use another non-unitary gauge. Such differences can be neglected for our purpose here. Of course including the other diagrams (with W/Z) will produce a gauge-invariant result.

with

$$A_1 = (\alpha_{2b}\alpha_{2s}^* m_b + \alpha_{1b}\alpha_{1s}^* m_s) f_1(t) + (\alpha_{2s}^*\alpha_{1b}) M_* f_2(t) \tag{48}$$
$$B_1 = (\alpha_{1b}\alpha_{1s}^* m_b + \alpha_{2b}\alpha_{2s}^* m_s) f_1(t) + (\alpha_{1s}^*\alpha_{2b}) M_* f_2(t)$$

and

$$f_1(t) = -\frac{t[t(t-6)+3] + 6t\ln(t) + 2}{12(t-1)^4}; \qquad f_2(t) = -\frac{(t-4)t + 2\ln(t) + 3}{2(t-1)^3} \tag{49}$$

where M_* is the mass of the heavy fermion, Q_U is the charge of the heavy fermion, $t = M_*^2/M_w^2$. This result can also be used for the diagram with *neutral* Higgs (including physical Higgs and the neutral would-be-Goldstone boson) in the loop.

The result for the second diagram(See Fig. 3 B), with photon attached to the charged Higgs, is

$$\mathcal{H}_2^{eff} = \frac{-ie}{8\pi^2}\frac{(2\epsilon\cdot p)}{M_w^2}\left\{A_2 \bar{s}(1+\gamma_5)b + B_2\bar{s}(1-\gamma_5)b\right\} \tag{50}$$

with

$$A_2 = (\alpha_{2b}\alpha_{2s}^* m_b + \alpha_{1b}\alpha_{1s}^* m_s) g_1(t) + (\alpha_{1b}\alpha_{2s}^*) M_* g_2(t) \tag{51}$$
$$B_2 = (\alpha_{1b}\alpha_{1s}^* m_b + \alpha_{2b}\alpha_{2s}^* m_s) g_1(t) + (\alpha_{1s}^*\alpha_{2b}) M_* g_2(t)$$

and

$$g_1(t) = \frac{2t^3 - 6t^2\ln(t) - 6t + 1 + 3t^2}{12(t-1)^4}; \qquad g_2(t) = \frac{t^2 - 2t\ln(t) - 1}{2(t-1)^3} \tag{52}$$

These results (Eq. 47 and 50) can be applied to calculate $\Gamma(b \to s\gamma)$ if we find the couplings α_{1i}, α_{2i} (see Eq. 46).

B Mass matrix diagonalization and dipole moment operator for one generation

Having performed a calculation of the dipole operator for $b \to s$ generated by general couplings of bottom and strange quarks to Higgs and heavy fermions, we now consider this contribution specifically in the two-site model. As explained in section 4.1, we have to consider the mixing between the SM and heavy fermions of all three generations induced after EWSB. Diagonalization of this mixing will give the couplings to Higgs in mass eigenstate basis for the quarks which we can then plug into the model-independent results of appendix A in order to calculate $b \to s\gamma$. In this section, we will first consider *analytically* the simpler *one* generation case, i.e., a calculation of $(g-2)_\mu$, which will be generalized (numerically) to the case of three generations for calculating

$b \to s\gamma$ in the next sub-section. This result for the dipole operator for one generation was also used in section 4.1 to obtain an *estimate* for $b \to s\gamma$ (after multiplying by an estimate for the generational mixing factors).

The one generation mass matrix for down type quarks (including effects of EWSB) is (see Eq. (15))

$$(\bar{b}_L \quad \bar{\tilde{B}}_L \quad \bar{B}_L) M_* \begin{pmatrix} x s_q s_b & 0 & x s_q \\ 0 & x & 1 \\ x s_b & 1 & x \end{pmatrix} \begin{pmatrix} \tilde{b}_R \\ B_R \\ \tilde{B}_R \end{pmatrix} + h.c. \tag{53}$$

where $x = vY_* / \left(M_* \sqrt{2}\right)$, $\tilde{B}$ and B are composite $SU(2)_L$ singlet and doublet fermions respectively. It can be diagonalized by bi-unitary transformation to first order in x.

$$O_{D_L} = \begin{pmatrix} 1 & x s_q/\sqrt{2} & -x s_q/\sqrt{2} \\ -x s_q & 1/\sqrt{2} & -1/\sqrt{2} \\ 0 & 1/\sqrt{2} & 1/\sqrt{2} \end{pmatrix}; \qquad O_{D_R} = \begin{pmatrix} 1 & x s_b/\sqrt{2} & x s_b/\sqrt{2} \\ -x s_b & 1/\sqrt{2} & 1/\sqrt{2} \\ 0 & 1/\sqrt{2} & -1/\sqrt{2} \end{pmatrix} \tag{54}$$

$$O^\dagger_{D_L} \begin{pmatrix} x s_q s_b & 0 & x s_q \\ 0 & x & 1 \\ x s_b & 1 & x \end{pmatrix} O_{D_R} = \mathrm{diag}(\ x s_q s_b\ , 1 + x\ , 1 - x\ ) \tag{55}$$

Similarly we can get the up-type diagonalization matrix (O_{U_L}) and (O_{U_R}). We define the mass eigenstates as

$$\begin{pmatrix} b_L^{\rm SM} \\ B_{1L} \\ B_{2L} \end{pmatrix} = O^\dagger_{D_L} \begin{pmatrix} b_L \\ \tilde{B}_L \\ B_L \end{pmatrix} \qquad \begin{pmatrix} b_R^{\rm SM} \\ B_{1R} \\ B_{2R} \end{pmatrix} = O^\dagger_{D_R} \begin{pmatrix} \tilde{b}_R \\ B_R \\ \tilde{B}_R \end{pmatrix}, \tag{56}$$

where $b^{\rm SM}$ is the SM bottom quark with mass $vY_* s_q s_b$. B_1 is the heavy state with mass $(1+x)M_*$ and B_2 is the heavy state with mass $(1-x)M_*$. Similar mass eigenstates can be defined for up-type quarks $(t^{\rm SM}, T_1, T_2)$.

The coupling between down type and up type quarks through charged Higgs is

$$Y_* (\bar{b}_L^{\rm SM} \quad \bar{B}_{1L} \quad \bar{B}_{2L})\ O^\dagger_{D_L} \begin{pmatrix} s_q s_t & 0 & s_q \\ 0 & -1 & 0 \\ s_t & 0 & 1 \end{pmatrix} O_{U_R} \begin{pmatrix} t_R^{\rm SM} \\ T_{1R} \\ T_{2R} \end{pmatrix} H^- \tag{57}$$

We can find the couplings between $b_L^{\rm SM}$ and heavy up-type quarks

$$Y_* H^- \bar{b}_L^{\rm SM} \left[\frac{(1+x)}{\sqrt{2}} s_q T_{1R} + \frac{(x-1)}{\sqrt{2}} s_q T_{2R} \right] \tag{58}$$

Similarly, we have the coupling coming from another chirality

$$Y_* (\bar{b}_R^{\rm SM} \quad \bar{B}_{1R} \quad \bar{B}_{2R})\ O^\dagger_{D_R} \begin{pmatrix} -s_q s_b & 0 & -s_b \\ 0 & 1 & 0 \\ -s_q & 0 & -1 \end{pmatrix} O_{U_L} \begin{pmatrix} t_L^{\rm SM} \\ T_{1L} \\ T_{2L} \end{pmatrix} H^- \tag{59}$$

which gives us the coupling

$$Y_* H^- \bar{b}_R^{SM} \left[-\frac{(1+x)}{\sqrt{2}} s_b T_{1L} + \frac{(x-1)}{\sqrt{2}} s_b T_{2L} \right] \tag{60}$$

Altogether, we have the charged Higgs coupling between SM bottom quark and heavy up-type quark

$$\begin{aligned} Y_* H^- \bar{b}^{\rm SM} \left[(\frac{1+\gamma_5}{2})(1+x)\frac{s_q}{\sqrt{2}} - (\frac{1-\gamma_5}{2})(1+x)\frac{s_b}{\sqrt{2}} \right] T_1 + \\ Y_* H^- \bar{b}^{\rm SM} \left[(\frac{1+\gamma_5}{2})\frac{x-1}{\sqrt{2}} s_q + (\frac{1-\gamma_5}{2})\frac{x-1}{\sqrt{2}} s_b \right] T_2 \end{aligned} \tag{61}$$

Based on our parametrization of the couplings (see Eq. 46), we extract (we ignore the subscript "b" in $\alpha_{1,2}$ here)

$$\begin{aligned} \alpha_1^{(1)} &= -\frac{(1+x)s_b}{2\sqrt{2}} Y_* \\ \alpha_1^{(2)} &= \frac{(x-1)s_b}{2\sqrt{2}} Y_* \\ \alpha_2^{(1)} &= \frac{(1+x)s_q}{2\sqrt{2}} Y_* \\ \alpha_2^{(2)} &= \frac{(x-1)s_q}{2\sqrt{2}} Y_* \end{aligned} \tag{62}$$

The contribution from heavy up-type quark to the dipole moment operator would be (see Eq. 47 and 50)

$$\mathcal{H}^{\rm dipole}_{\rm charged\ Higgs} = \frac{ie}{8\pi^2} \frac{(2\epsilon \cdot p)}{M_w^2} K \left[\bar{b}^{\rm SM}(1-\gamma_5) b^{SM} + \bar{b}^{\rm SM}(1+\gamma_5) b^{\rm SM} \right] \tag{63}$$

with

$$K = \sum_{i=1}^{2} \left(|\alpha_1^{(i)}|^2 + |\alpha_2^{(i)}|^2 \right) m_b \left[\frac{2}{3} f_1(t_i) - g_1(t_i) \right] + \sum_{i=1}^{2} (\alpha_1^{(i)*} \alpha_2^{(i)}) M_i \left[\frac{2}{3} f_2(t_i) - g_2(t_i) \right] \tag{64}$$

Substituting Eq. (62) in (64) one can see that the first term is sub-leading due to additional powers of s_b,s_q. For the second term we use the approximation

$$\frac{2}{3} f_2(t_i) - g_2(t_i) \approx -\frac{5}{6} \frac{M_w^2}{(M_*)^2 (1 \pm x)^2} \tag{65}$$

It gives us

$$K \approx \frac{5x}{24} s_q s_b \frac{M_w^2}{(M_*)^2} (Y_*)^2 \tag{66}$$

And the final result is

$$\mathcal{H}^{\rm dipole}_{\rm charged\, Higgs} = \frac{5}{12} (Y_*)^2 m_b \frac{ie}{16\pi^2} \frac{(2\epsilon \cdot p)}{(M_*)^2} [\bar{b}^{\rm SM}(1-\gamma_5) b^{SM} + \bar{b}^{SM}(1+\gamma_5) b^{\rm SM}] \tag{67}$$

Note that we have chosen *not* to combine the two terms in $\Big[...\Big]$ in the above equation. The reason is that when we apply the above result to $b \to s\gamma$, then the two terms with *different* chirality structure will be multiplied by different mixing angles and hence it is useful to keep track of the two terms separately even for the case of one generation.

The contribution from neutral Higgs can be calculated in a similar fashion. The coupling between down-type quarks and neutral Higgs is

$$Y_* H^0 \left(\bar{b}_L^{\rm SM} \quad \bar{B}_{1L} \quad \bar{B}_{2L}\right) O_{D_L}^\dagger \begin{pmatrix} s_q s_b & 0 & s_q \\ 0 & 1 & 0 \\ s_b & 0 & 1 \end{pmatrix} O_{D_R} \begin{pmatrix} b_R^{\rm SM} \\ B_{1R} \\ B_{2R} \end{pmatrix} + h.c. \tag{68}$$

From this we can find the coupling between SM b quark and heavy down-type fermions:

$$Y_* H^0 \left\{ \bar{b}_L^{\rm SM} \left[\frac{1-x}{\sqrt{2}} s_q B_{1R} - \frac{1+x}{\sqrt{2}} s_q B_{2R} \right] + \bar{b}_R^{\rm SM} \left[\frac{1-x}{\sqrt{2}} s_b B_{1L} + \frac{1+x}{\sqrt{2}} s_b B_{2L} \right] \right\} + h.c. \tag{69}$$

which gives us (see Eq. 46)

$$\begin{aligned} \alpha_1^{(i)} &= Y_* \frac{s_b}{2\sqrt{2}} (1-x,\ 1+x) \\ \alpha_2^{(i)} &= Y_* \frac{s_q}{2\sqrt{2}} (1-x,\ -1-x) \end{aligned} \tag{70}$$

Follow the same procedure as before, including only the first diagram (Fig. 3A). We get

$$\mathcal{H}^{\rm dipole}_{\rm neutral\, Higgs} = -\frac{1}{4} (Y_*)^2 m_b \frac{ie}{16\pi^2} \frac{(2\epsilon \cdot p)}{(M_*)^2} [\bar{b}^{\rm SM} (1-\gamma_5) b^{SM} + \bar{b}^{\rm SM} (1+\gamma_5) b^{\rm SM}] \tag{71}$$

B.1 Three generation calculation

Generalizing to three generations, the mass matrix Eq. (53) becomes 9×9. However, since analytical diagonalization of this 9×9 matrix is difficult, we do it numerically and extract the parameters α_1, α_2 (see Eq. (46) which parametrize general interaction between fermions and Higgs field, keeping in mind that $\alpha_{1,2}$ will now have six components $\alpha_{1,2}^{(1,2,...6)}$ because we have six heavy mass eigenstates). Then using these α's in the formulae from the loop calculation in Eqs. (47) and (50), we will get *exact* values for the C_7 and C_7' coefficients in the amplitude for $b \to s\gamma$ (instead of the estimates presented in section 4.1). Similarly, applying the above diagonalization to Eq. (16) allows us to calculate the flavor-violating couplings of heavy gluon to the SM fermions *after* EWSB (including effects of SM-heavy fermion mixing) which generate contributions to ϵ_K. The results of the numerical scan in section 6 are based on these calculations.

C Details of Scan

All the masses and mixings in the fermion sector (including SM and heavy) can be parametrized by the composite site Yukawa couplings ($Y^*_{u,d}$) and the elementary/composite mixings ($s_{q,d,u}$). Of course, we must choose Y_* and $s_{q,u,d}$ to give the observed quark masses and CKM angles. We would like the composite site Yukawa couplings to be "anarchical", i.e., of the same order, and $s_{q,d,u}$ to be hierarchical[10] in order to explain SM fermion masses and mixing. This anarchy condition and Eqs. (20) and (21) (with generalization to other quark masses) lead to the following rough size of the mixing angles

$$\begin{aligned} s_{u3} &\sim 1, \quad s_{d3} \sim \frac{s_{u3} m_b Y_*^u}{m_t Y_*^d}, \quad s_{q3} \sim \frac{m_t \sqrt{2}}{v s_{u3} Y_*^u}, \\ s_{d2} &\sim \frac{m_s s_{d3}}{m_b \lambda^2}, \quad s_{u2} \sim \frac{s_{u3} m_c}{\lambda^2 m_t}, \quad s_{q2} \sim \lambda^2 s_{q3}, \\ s_{d1} &\sim \frac{m_d s_{d3}}{m_b \lambda^3}, \quad s_{u1} \sim \frac{m_u s_{u3}}{m_t \lambda^3}, \quad s_{q1} \sim \lambda^3 s_{q3}. \end{aligned} \tag{72}$$

We choose to scan over the following independent variables

- Elementary-composite mixing angles $s_{q,u,d}$
- SM rotation matrices U_R, U_L, D_R (D_L is fixed by $D_L = U_L \cdot V_{CKM}$)

(This choice is equivalent to treating $Y_*^{u,d}$ and $s_{q,u,d}$ as the independent variables which are scanned.) We randomly vary each set of the independent variables around their "natural" size by a factor of three, where the natural sizes for the $s_{q,u,d}$ are defined to be Eq. (72) and that for U_R, U_L, D_R in Eq. (20) by replacing "$\sim$" by "$=$" in both these equations. Then we calculate corresponding $Y_{*u,d}$[11]

$$\begin{aligned} Y_u = \tfrac{\sqrt{2}}{v}(U_L) \cdot M_u^{diag} \cdot (U_R)^\dagger; \qquad Y_d = \tfrac{\sqrt{2}}{v}(D_L) \cdot M_d^{diag} \cdot (D_R)^\dagger \\ Y_*^{u,d} \approx s_Q^{-1} Y_{u,d} s_{u,d}^{-1} \end{aligned} \tag{73}$$

Then we check whether our $Y_{*u,d}$ are "anarchical", i.e., whether they satisfy the following condition

$$\begin{aligned} \frac{\text{Max}(|Y_{*u}|)}{3} < \text{G.M.}(|Y_{*u}|) < 3 * \text{Min}(|Y_{*u}|) \\ \frac{\text{Max}(|Y_{*d}|)}{3} < \text{G.M.}(|Y_{*d}|) < 3 * \text{Min}(|Y_{*d}|) \end{aligned} \tag{74}$$

where G.M. stands for the geometrical mean. If these Yukawas satisfy "anarchy" condition, we proceed to calculate new physics contribution to $\Gamma(b \to s\gamma)$, $\text{Im}\, C_4^K$ (as described in section B.1) and $\delta g_{Z\bar{b}_L b_L}$ as in Eq. (44). On the other hand, if these Yukawas do not satisfy the anarchy condition, then we discard them. We have checked that the couplings ($Y_{*u,d}$) generated in this way are random, i.e., that there is no correlation between different elements of the matrices. The results of the scan are presented in Fig. 5 to 10.

---

[10] As mentioned earlier, these assumptions can be justified by the correspondence with the $5D$ model to be discussed later.

[11] We are ignoring the mixing between the SM and heavy fermions induced by EWSB in the last relation here which results in an error of $Y_*^2 v^2 / M_*^2 \sim$ a few % (for the our choice of parameters) in the determination of Y_*.

D Sub-leading effects

D.1 ϵ_K

Similarly to the heavy gluon exchange, heavy EW gauge boson exchange generates $(V-A)\times(V+A)$ operators, but it gives $C_5\,(M_*)$ only and of smaller size than $C_4\,(M_*)$ from heavy gluon due to smaller values of gauge couplings and gauge quantum numbers in the heavy EW boson exchange than in heavy gluon exchange. Moreover, the model-*independent* constraint from UTfit [35] on C_5 (renormalized at a few TeV scale) is weaker than for C_4. So, we find that constraint on M_* from heavy EW gauge boson exchange in the two-site model is weaker than that from heavy gluon exchange: see also discussion in [15].

We have also checked that the constraint from $(V-A)\times(V-A)$ and $(V+A)\times(V+A)$-type operators from heavy gauge boson exchange in the two-site model can be weaker than from $(V-A)\times(V+A)$ operator from heavy gluon exchange. In detail, such exchange generates the Wilson coefficient $C_1\,(M_*)$. Firstly, the model-independent bound on C_1 (renormalized at a few TeV scale) is weaker than for C_4 due to the absence of matrix element *and* RGE enhancement for C_1 relative to C_4. Secondly, in the two-site model, the size of C_1 can be effectively *controlled* by a single parameter, namely, the amount of elementary-composite mixing of b_L – the point being that the other down-type elementary-composite mixings are then fixed: the ones for d_L, s_L via CKM mixing angles and then, for given composite Yukawa, the right-handed ones by SM Yukawa (as discussed earlier).[12] Usually, one chooses s_{q3} to satisfy the constraint from $Zb\bar{b}$ (as discussed earlier) and simultaneously to obtain the correct top Yukawa, i.e., $Y_* s_{q3} \sim O(1)$, assuming SM t_R is fully composite. For the choice of $M_* \sim$ a few TeV and $Y_* \sim$ a few, we then find $s_{q3} \sim 1/$ (a few). With this size of s_{q3} and once we choose M_* to satisfy the ϵ_K-constraint from $(V-A)\times(V+A)$ operators, we find that both $(V-A)\times(V-A)$ and $(V+A)\times(V+A)$-type operators do not give as strong a constraint as from heavy gluon contribution to the $(V-A)\times(V+A)$ operator: see also [15] for a related discussion.

D.2 Other B-physics observables

It is easy to compute $B_{d,\,s}$ mixing amplitudes in the two-site model. The main new physics contribution comes from the flavor violating couplings of heavy gluon, just like for $\Delta S = 2$ process discussed earlier. We have checked that bounds on $B_{d,\,s}$ mixing amplitude is satisfied once ϵ_K is safe: see also [16, 17, 14, 15] for related discussions.

In detail, the $(V-A)\times(V+A)$ type operator generated in the two-site model is less constrained in the $B_{d,\, s}$ systems than in the K system for the following reasons. Firstly, the model-independent constraint on $C^{new}_{4,\, 5}\left(M_*\right)/C^{SM}_1\left(M_W\right)$ is weaker in the $B_{d,\, s}$ system than in the K system since there is no matrix element enhancement for $C_{4,5}$ in the $B_{d,\, s}$ mixing operators (unlike for K mixing). Secondly, in the two-site model, the size of $C^{new}_{4,\, 5}\left(M_*\right)/C^{SM}_1\left(M_W\right)$ for $B_{d,\, s}$ mixing turns out (due to the particular values of down-type quark masses) to be smaller than in K mixing. For the $(V \pm A) \times (V \pm A)$ type operator, the analysis is similar to that for K mixing.

---

[12] Contrast this case to that for $C_{4,\,5}$ above whose size was *fixed* in terms of SM fermion Yukawa couplings/masses (due to a combination of left and right-handed elementary-composite mixings involved in C_4).

Besides $\Delta F = 2$ processes, there are also new physics contribution to $\Delta F = 1$ processes in the two-site model. For example, the non-universal shift (in gauge eigenstate basis) in the Z couplings for b_L (vs. d_L, s_L) will lead to flavor-violating couplings to Z once we transform to mass eigenstate basis, resulting in the (flavor-violating) processes $b \to s f \bar{f}$, where f = quark, lepton. We have checked that the new physics contribution to $b \to s l^+ l^-$ process is below the experimental bound once we satisfy $\delta g_{Z \bar{b}_L b_L}/g_{Z \bar{b}_L b_L} \lesssim 0.25\%$ as required by the flavor-preserving $Zb\bar{b}$ data: see also [24] for a related discussion.

We also checked the new physics contribution to the time-dependent CP asymmetry in $b \to s\gamma$, i.e., S_{CP} which requires an interference between the C_7 and $C^\prime_7$ amplitudes: $S_{CP} \sim C^\prime_7 C_7/(|C_7|^2 + |C^\prime_7|^2)$. In the SM, $S_{CP} \sim m_s/m_b$ due to the suppression of $C^\prime_7$ by m_s/m_b relative to C_7 [43]. In the two-site model, new physics contribution will generically give $C^\prime_7 \sim C^{SM}_7$ so that we expect S_{CP} to be sizable in the two-site model. However, we found that there is no significant constraint coming from S_{CP} because of the large experimental uncertainty at present [44].

E Relation to $5D$ AdS Model

The two-site model can be considered to be a deconstruction of the $5D$ AdS model with the following metric:

$$\begin{aligned} (ds)^2 &= e^{-2ky} dx^\mu dx_\mu + (dy)^2 \qquad (0 \leq y \leq \pi R) \\ &\equiv \frac{1}{(kz)^2}\left(dx_\mu dx^\mu + dz^2\right) \qquad (z_h \leq z \leq z_v) \end{aligned} \tag{75}$$

where $z \equiv e^{ky}/k$, and with the two endpoints $z_h \equiv 1/k$ and $z_v \equiv e^{k\pi R}/k$ being denoted by the Planck and the TeV branes, respectively. The curvature scale k is taken to be of the order of the $4D$ Planck scale (M_{Pl}) and we choose $k\pi R \sim \log\left(M_{Pl}/\text{TeV}\right)$ with the SM Higgs being localized near the TeV brane in order to solve the Planck-weak hierarchy problem. The KK masses are quantized in units of $\sim ke^{-k\pi R} \sim$ TeV and are localized near the TeV brane. The composite site of the two-site model corresponds (roughly) to the TeV brane and elementary site to the Planck brane (but moved close to the TeV brane with renormalization of the interactions localized on it, i.e., as per holographic RG flow [45]). The mass eigenstates of the two-site model *before* EWSB (which are admixtures of elementary and composite site particles) correspond to the zero and KK modes in the $5D$ model[13] (again with Higgs vev set to zero), i.e.,

$$\begin{aligned} \text{SM states} \quad &\leftrightarrow \quad \text{zero modes} \\ \text{heavy states} \quad &\leftrightarrow \quad \text{KK modes} \end{aligned} \tag{76}$$

Here, we show the correspondence between the couplings of the two-site and the $5D$ AdS model. For more discussion on this issue, see reference [30].

E.1 Size of composite gauge coupling

Since g_* is the composite site coupling, i.e., the coupling of composite sector ($\approx$ heavy) gauge bosons to the composite sector ($\approx$ heavy) fermions, it should correspond (roughly) to the coupling of single gauge KK mode to two KK fermions. We find that this coupling in the $5D$ model is (roughly) given by $g_5\sqrt{k}$, where g_5 is the dimensionful $5D$ gauge coupling. This result is (almost) independent of the range of profiles of KK fermions that is of interest for down-type quarks (see section E.2). Hence, we identify:

$$g_* \quad \leftrightarrow \quad g_5\sqrt{k} \tag{77}$$

E.1.1 Matching to QCD coupling

The value of the 5D coupling $g_5\sqrt{k}$ can be fixed by matching it to the $4D$ QCD coupling [46, 47]:

$$\frac{1}{g^{QCD\,2}} \quad \approx \quad \log\left(M_{Pl}/\text{TeV}\right)\left(\frac{1}{\left(g_5^{QCD\,2}k\right)}+\frac{b^{QCD}}{8\pi^2}\right)+\frac{1}{g_{Planck}^{QCD\,2}}+\frac{1}{g_{TeV}^{QCD\,2}} \tag{78}$$

where $1/g^{QCD\,2}_{Planck,\,TeV}$ are the bare/tree-level (positive) brane-kinetic terms and the $b^{QCD}\approx -7$ is the result of one-loop running effects. So using $g^{QCD}\sim 1$ (renormalized at the TeV scale) we get

- $g_5\sqrt{k}\sim 3$ for matching at the *loop* level, i.e., including the b^{QCD} term with zero bare/tree-level brane kinetic terms and with a Planck-weak hierarchy. Clearly, this is the *smallest* allowed value of g_* for this hierarchy.

- $g_5\sqrt{k}\sim 6$ for matching at the *tree*-level, i.e., neglecting the b^{QCD} term, with no brane kinetic terms[14].

---

[13] These modes are non-vanishing on *both* the Planck and the TeV branes, corresponding to the admixtures in the two-site model.

[14] Equivalently, choosing the tree-level brane kinetic term to cancel the loop contribution": see discussion in [14].

In general, the value of $g_5\sqrt{k}$ can be even larger than above if we allow non-zero (positive) brane kinetic terms (on the Planck or TeV brane). In particular, with non-zero *Planck* brane localized kinetic terms, the couplings of (lightest) gauge KK are still set by $g_5\sqrt{k}$ since these modes are localized near TeV brane. Thus, the KK coupling (measured in units of SM gauge coupling) also increases as these brane kinetic terms are increased. On the other hand, allowing (sizable) *TeV* brane localized kinetic terms has a more interesting effect as follows. The value of $g_5\sqrt{k}$ (again measured in units of the SM gauge coupling) increases as in the case of the Planck brane localized kinetic terms, but the KK gauge coupling is clearly determined by the kinetic term localized on the TeV brane where the KK modes are localized (instead of being set by $g_5\sqrt{k}$). As the size of the brane kinetic terms increases, it turns out that the gauge KK coupling (measured in units of the SM gauge coupling as usual) becomes weaker [29]. At the same time, the mass of the lightest KK mode becomes smaller in such a way that ratio

$$\frac{\text{KK coupling constant}}{\text{Lightest KK mass in units of } ke^{-k\pi R}} \tag{79}$$

stays roughly the same (for moderately large brane terms), up to $O(1)$ factors. The flavor-violating amplitude (in units of $ke^{-k\pi R}$) depends on precisely the above ratio. So it is clear that large TeV brane terms can allow lighter KK states to satisfy the flavor constraints, but it will *not* allow a reduction in the scale $ke^{-k\pi R}$ which might be the one more relevant (than the lightest KK mass scale) for the fine tuning in EWSB. Although a detailed analysis of TeV brane kinetic terms is beyond the scope of this paper, it is important to keep in mind that such terms can affect the bounds on the scale $ke^{-k\pi R}$ by $O(1)$ factors. Finally, for smaller than Planck-weak hierarchy, for example as in the "Little Randall-Sundrum model" [48], it is clear that $g_5\sqrt{k}$ can be smaller as seen from Eq. (78).

E.1.2 Perturbativity bound on size of $5D$ gauge coupling

On the other hand, an *upper* bound on g_5^{QCD} coupling can also be obtained from the condition of perturbativity of the $5D$ QCD theory in the following way. We can estimate the loop expansion parameter for this theory by comparing the one-loop correction to the tree-level value of a coupling (or comparing a two-loop correction to a one-loop effect). This loop expansion parameter grows with energy (or number of active KK modes) due to the non-renormalizability of $5D$ couplings. So, the number of KK modes below the $5D$ cut-off, denoted by N_{KK}, can then be estimated by setting this loop expansion parameter to be ~ 1 (see, for example [49]). As an example, we can *estimate* the one-loop correction to the tree-level value of the three KK gluon coupling arising from this interaction itself. Including color and helicity factors of ~ 3 each for this loop diagram (see, for example, reference [47]), we find:

$$\frac{\left(g_5^{QCD}\sqrt{k}\right)^2 3\times 3}{16\pi^2} N_{KK} \quad \sim \quad 1 \tag{80}$$

where $\sim \left(g_5^{QCD}\sqrt{k}\right)$ is coupling of 3 KK gluons and the single power of N_{KK} (i.e., single KK sum) follows from KK number conservation at the purely KK gluon vertices. Equivalently, the dimension of g_5^{QCD} being $-1/2$ implies that the $5D$ loop expansion parameter is $\sim (g_5^{QCD})^2 E/\left(16\pi^2\right)$ with $E/k \sim$ being the number of active KK modes.

We can also instead consider the one-loop self-corrections to the coupling of KK gluon to two KK fermions, where the helicity factor of 3 is absent (in this sense, the estimate in Eq.(80) is conservative). The estimate in Eq. (80) leads to the following values of the number of KK modes below cutoff:

- $N_{KK} \sim 2$ for $g_5^{QCD}\sqrt{k} \sim 3$ which is again the smallest $g_5^{QCD}\sqrt{k}$ allowed for Planck-weak hierarchy (i.e., with loop-level matching of the $5D$ coupling to the $4D$ coupling and with no bare/tree-level brane kinetic terms).
- Whereas for $g_5^{QCD}\sqrt{k} \sim 6$ (i.e., with tree-level matching of the $5D$ coupling to the $4D$ coupling with no brane kinetic terms), there seems to be hardly any energy regime where the $5D$ theory is weakly coupled, i.e., $N_{KK} < 2$.

This conclusion about perturbativity for the $g_5^{QCD}\sqrt{k} \sim 6$ case is valid even if we do *not* include the helicity factor of ~ 3 as would be the case for the estimate of loop expansion parameter using the KK gluon coupling to two KK fermions (instead of coupling of three KK gluon coupling). So with this perturbativity motivation (and using the correspondence in Eq. 77), we have focused on using $g_{s*} \sim 3$ in our analysis of the two-site model, but of course, one should understand that these conclusions are just estimates.

E.2 Formulae for zero-mode and KK Yukawa and KK gauge couplings

We give some useful formulae for profiles of zero-mode fermion, KK fermion, gauge KK mode and bulk Higgs in $5D$ AdS model, neglecting (for simplicity) brane kinetic terms[15] (see, for example, reference [13] for fermion and gauge profiles and [26] for Higgs profile).

---

[15] Since the KK modes are localized near the TeV brane, localized kinetic terms there affect the KK decomposition and generate additional flavor-violating couplings of gauge KK modes to fermion zero-modes (see, for example, reference [19]). However, we assume that these brane terms are of size generated by loop-level bulk effects (which is a technically natural choice) so that these effects can be neglected for our purposes, as long as the bulk loops are perturbative.

First, we decompose the 5D fermion field as

$$\Psi(x,z) = \sum_n \psi^{(n)}(x)\chi_n(c,z) \tag{81}$$

where c is the ratio between $5D$ fermion mass term and AdS curvature scale k. The normalization condition for profiles is

$$\int_{z_h}^{z_v} dz \left(\frac{z_h}{z}\right)^4 \chi_n^2(c,z) = 1 \tag{82}$$

The fermion zero mode profile is

$$\chi_0(c,z) = f(c)\left(\frac{z}{z_h}\right)^{2-c} \frac{1}{\sqrt{z_h}} \left(\frac{z_h}{z_v}\right)^{1/2-c} \tag{83}$$

with

$$f(c) = \sqrt{\frac{1-2c}{1-(z_v/z_h)^{2c-1}}} \tag{84}$$

The KK fermion profile *for the same chirality as the zero-mode* is

$$\chi_n(c,z) = \left(\frac{z}{z_h}\right)^{5/2} \frac{1}{N_n^\chi \sqrt{\pi r_c}} [J_\alpha(m_n z) + b_\alpha(m_n) Y_\alpha(m_n z)] \tag{85}$$

with $\alpha = |c+1/2|$, m_n and b_α are given by

$$\frac{J_{\alpha\mp1}(m_n z_h)}{Y_{\alpha\mp1}(m_n z_h)} = \frac{J_{\alpha\mp1}(m_n z_v)}{Y_{\alpha\mp1}(m_n z_v)} = -b_\alpha(m_n) \tag{86}$$

with upper (lower) signs for $c > -1/2$ ($c < -1/2$) and normalization condition gives

$$|N_n^\chi|^2 = \frac{1}{2\pi r_c z_h}\left[z_v^2[J_\alpha(m_n z_v) + b_\alpha(m_n) Y_\alpha(m_n z_v)]^2 - z_h^2[J_\alpha(m_n z_h) + b_\alpha(m_n) Y_\alpha(m_n z_h)]^2\right] \tag{87}$$

It is useful to note that the ratio of zero and KK fermion profile at TeV brane is

$$\frac{\chi_0(c,z_v)}{\chi_n(c,z_v)} \approx \frac{f(c)}{\sqrt{2}} \tag{88}$$

Similarly, we perform KK decomposition for gauge bosons:

$$\mathcal{A}_\mu(x,z) = \sum_n A^{(n)}(x) f_n(z) \tag{89}$$

The gauge KK wavefunction is:

$$f_n(z) = \sqrt{\frac{1}{z_h}} \frac{z}{N_n^f} [J_1(m_n z) + b_n Y_1(m_n z)] \tag{90}$$

where b_n and gauge KK masses are fixed by:

$$\frac{J_0(m_n z_h)}{Y_0(m_n z_h)} = \frac{J_0(m_n z_v)}{Y_0(m_n z_v)} = -b_n \tag{91}$$

and the normalization condition

$$\int_{z_h}^{z_v} dz \left(\frac{z_h}{z}\right) f_n^2(z) = 1 \tag{92}$$

gives us

$$|N_n^f|^2 = \frac{1}{2}\left[z_v^2[J_1(m_n z_v) + b_n Y_1(m_n z_v)]^2 - z_h^2[J_1(m_n z_h) + b_n Y_1(m_n z_h)]^2\right] \tag{93}$$

The KK decomposition for a $5D$ scalar (bulk Higgs) is (here $\beta = \sqrt{4+\mu^2}$, with μ being the bulk Higgs mass in units of k):

$$\mathcal{H}(x,z) = v(\beta, z) + \sum_n H^{(n)}(x)\phi_n(z) \tag{94}$$

where $v(\beta, z)$ is the Higgs *vev* profile, which is very close to the (lightest) *physical* Higgs profile when $m_h \ll M_{KK}$. This profile can be chosen to be peaked near the TeV brane:

$$v(\beta, z) = v_4 z_v \sqrt{\frac{2(1+\beta)}{z_h^3(1-(z_h/z_v)^{2+2\beta})}} \left(\frac{z}{z_v}\right)^{2+\beta}. \tag{95}$$

The couplings between fermion zero modes and Higgs (Y_0), fermion KK modes and Higgs (Y_{KK}), fermion zero modes and gauge KK modes (g_{KK}) are given by overlap integrals of the their profiles multiplied by the $5D$ couplings:

$$\begin{aligned} Y_0\left(c_L, c_R, \beta\right) &= Y_5^{bulk} \int dz \left(\frac{z_h}{z}\right)^5 v(\beta, z)\chi_{0L}(c_L, z)\chi_{0R}(c_R, z)/v_4 \\ Y_{KK}\left(c_L, c_R, \beta\right) &= Y_5^{bulk} \int dz \left(\frac{z_h}{z}\right)^5 v(\beta, z)\chi_{nL}(c_L, z)\chi_{mR}(c_R, z)/v_4 \\ g_{KK}\left(c_L\right) &= g_5 \int dz \left(\frac{z_h}{z}\right)^4 f_n(z)\chi_{0L}(c_L, z)\chi_{0L}(c_L, z) \end{aligned} \tag{96}$$

where Y_5^{bulk} is defined by $\mathcal{S} \ni \int d^4x dz \sqrt{G}\, Y_5^{bulk} H(x,z)\overline{\Psi(x,z)}\Psi'(x,z)$ (with Ψ and Ψ' being $SU(2)_L$ doublet/singlet and G is the determinant of the metric) and has mass dimension $-1/2$ just like g_5. Again, Y_{KK} defined above is for KK modes with same chirality as the zero-mode. A similar expression can be obtained for the overlap integrals giving the coupling between KK gluon and two KK fermions which was used to obtain Eq. (77).

It is useful to know approximate formulae for these overlap integrals [13][14]. For example

$$g_{KK} \approx \left(g_5\sqrt{k}\right)\left(-\frac{1}{k\pi r_c} + f(c_L)f(c_R)\right) \tag{97}$$

where pre-factor of "1" that multiplies $f(c_L)f(c_R)$ is almost c-independent for $0.4 \lesssim c \lesssim 0.7$ that is of interest for down-type quarks.

Similarly, we define the parameter $a(\beta, c_L, c_R)$ by

$$Y_0\left(c_L, c_R, \beta\right) = a(\beta, c_L, c_R) Y_{KK}\left(c_L, c_R, \beta\right) f(c_L) f(c_R) \tag{98}$$

We find (numerically) that, for fixed Higgs vev profile, the $c_{L,R}$ dependence of a is *very* mild for the range $0.4 \lesssim c \lesssim 0.7$ that is of interest for the down-type quarks and hence we set $c_L = c_R = 0.55$ henceforth when we quote values of a. We give a table for a vs. the parameter β of bulk Higgs (see Table 1). We see that $a \sim O(1)$ as expected. In detail, the Higgs and KK fermion profiles are localized near the TeV brane so that Y_{KK} is dominated by overlap of profiles in this region. So, we get $Y_{KK} \sim Y_5\sqrt{k}$ (with a mild dependence on c and β), where the $5D$ Yukawa is made dimensionless simply by a factor of $\sim \sqrt{k}$ coming from the normalized profiles at the TeV brane: see Eqs. (85) and (95). Even though the fermion zero-modes (except for top quark) are localized near the Planck brane, their overlap with the Higgs is still dominated by the region near the TeV brane for the choices of c's relevant for quark masses[16]. Therefore, using the ratio of fermion zero and KK mode profiles (f's) given in Eq. (88), we expect $Y_0 \sim Y_{KK} f(c_L) f(c_R) \sim \left(Y_5\sqrt{k}\right) f(c_L) f(c_R)$, i.e., $a \sim O(1)$. Note that $f(c)$'s can be hierarchical even with small variations in c's, resulting in a solution to the flavor hierarchy problem in the sense that $4D$ Yukawa matrix (Y_0) can be hierarchical without any (large) hierarchies in the $5D$ theory, i.e., with anarchic $5D$ Yukawa matrix (or Y_{KK}) and $O(1)$ c's.

β	a	M_{KK} ($g_5^{QCD}\sqrt{k} = 3$, $Y_{KK} = 6$)	M_{KK} ($g_5^{QCD}\sqrt{k} = 6$, $Y_{KK} = 6$)
0	1.5	3.7 TeV	7.4 TeV
1(two-site)	1	5.5 TeV	11 TeV
2	0.75	7.3 TeV	14.6 TeV
∞ (brane)	0.5	11 TeV	22 TeV

Table 1: The values of the parameter a (relating zero to KK mode Yukawa couplings: see Eq. (98)) in 1st column for different values of the parameter β (2nd column) which determines the profile of the bulk Higgs (Eq. (95)). The two-site model and brane Higgs case are also shown as corresponding to specific values of β (see discussion in text). The bound on M_{KK} (from ϵ_K *only*, based on the estimate in Eq. (103)) for the purely composite sector (or KK) gauge coupling $g_5^{QCD}\sqrt{k} = 3$ (3rd column) and $g_5^{QCD}\sqrt{k} = 6$ (last column) are also shown. We fix the composite/KK Yukawa coupling $Y_{KK} = 6$ for all entries in the table and $c_L = c_R = 0.55$ in order to obtain the value of a.

The following observation about the parameter a is crucial for the analysis of ϵ_K in next section. Since the fermion zero modes profiles peak near the Planck brane while the fermion KK mode profiles peak near the TeV brane, it is clear that the overlaps of profiles of fermion zero modes with Higgs increase while those of fermion KK modes with Higgs decrease as the Higgs wavefunction moves farther *away* from the TeV brane. Therefore, as seen from this table,

- as we *decrease* the parameter β determining the Higgs profile in Eq. (95) – thereby localizing the Higgs away from the TeV brane, the parameter a in Eq. (98) *increases.*

---

[16] For larger values of c's (i.e., fermion zero-modes localized closer to the Planck brane) as relevant for Dirac neutrino masses, the overlaps with Higgs can be dominated by the region near the Planck brane instead [50].

We thus expect the opposite limit, $\beta \to \infty$, to reproduce brane Higgs scenario. In fact, for brane-localized Higgs, couplings of fermions to Higgs are simply given by wavefunctions of fermions at TeV brane, i.e., there is *no* overlap integral to be performed:

$$\begin{aligned} Y_0^{brane} &= \left(Y_5^{brane} k\right) f_L f_R \\ Y_{KK}^{brane} &= \left(2 Y_5^{brane} k\right) \end{aligned} \tag{99}$$

with $\mathcal{S} \ni \int d^4x \sqrt{G} Y_5^{brane} H(x) \overline{\Psi_L(x, z_v)} \Psi_R'(x, z_v)$. Note that dimension of Y_5 changes from $-1/2$ to -1 as we switch from bulk Higgs to brane-localized Higgs. The factor of two in Y_{KK}^{brane} in second line of Eq. (99) comes from the fact that the normalized KK wavefunction at TeV brane is $\approx \sqrt{2k}$ (see Eq. (85)). From Eqs. (98) and (99), the model with brane-localized Higgs (effectively) has $a = 1/2$. And, the numerical calculation of the overlap integrals for bulk Higgs shows that indeed $a \to 1/2$ for $\beta \to \infty$ (see Table 1), in agreement with the above expectation.

Now we can see the similarity between the two-site model and the bulk Higgs scenario. First, we compare the gauge couplings between the two cases: Eq. (97) and $\mathcal{L}^{SM-SM}$ term of Eq. (16), using Eq. (77). From these equations, we can make the following identifications:

$$\begin{aligned} s_{L,R} &\leftrightarrow f_{L,R} \\ \frac{1}{k\pi r_c} &\leftrightarrow \tan^2\theta \end{aligned} \tag{100}$$

As mentioned above, f_{L_i,R_i} can be hierarchical with small variations in $5D$ fermion mass parameters (c). Therefore, our choice of hierarchical elementary/composite mixing angles ($s_{q,u,d}$) in the two-site model is justified.

We turn to Yukawa couplings and compare Eq. (98) with $\mathcal{L}_Y^{\text{SM-SM}}$ term of Eq. (15). First, just like for the gauge couplings, we should identify the Higgs coupling to heavy fermions in the two-site model with the Higgs coupling to KK fermions in the $5D$ model[17], i.e.,

$$Y_* \leftrightarrow Y_{KK} \tag{101}$$

(In particular, both are assumed to be anarchic.) Then we can see that the two-site and $5D$ Yukawa coupling equations match if $a = 1$. Therefore, we conclude that

- the two-site model "mimics" the bulk Higgs scenario with $\beta \approx 1$ (which has $a \approx 1$). This result is also shown in Table 1.

---

[17] Note that, for a fixed β, Y_{KK} is only mildly sensitive to $c_{L,\,R}$'s.

E.3 Bound from ϵ_K

Following the arguments of the analysis of ϵ_K for the two-site model, it is clear that, in the bulk Higgs scenario, we get from KK gluon exchange

$$C_{4\,\text{estimate}}^{5D}\left(M_{KK}\right) \;=\; \frac{\left(g_5\sqrt{k}\right)^2}{Y_{KK}^2 a\,)(\beta)^2}\frac{2m_s m_d}{v^2}\frac{1}{M_{KK}^2}, \tag{102}$$

where "estimate" has the same meaning as in our analysis of the two-site model. Thus the constraint from ϵ_K is

$$M_{KK} \gtrsim 11\frac{g_5\sqrt{k}}{Y_{KK}a(\beta)}\text{TeV} \tag{103}$$

The bounds on M_{KK} for different values of β (i.e., choices of Higgs profiles), including the brane Higgs case and the two-site model is shown in Table 1 for $g_5^{QCD} = 3, 6$ and $Y_{KK} = 6$.

Now we can compare our results to previous analysis: references [14, 15] used a brane-localized Higgs, i.e., $a \sim 1/2$, with $Y_5^{brane}k \sim 3$, i.e., $Y_{KK} \sim 6$ (from Eq. 99). They obtained the bound on KK scale of $\sim 20(10)$ TeV for the case of $g_5^{QCD}\sqrt{k} \sim 6(3)$ which agrees with our results in Table 1. However, from Table 1, we see that

- for *same* $g_5\sqrt{k}$ and KK Yukawa (Y_{KK}), the bound on M_{KK} from ϵ_K is lowered for a *bulk* Higgs (instead of brane-localized Higgs).

Of course, this reduction in the KK scale for a bulk Higgs relative to the case of brane localized Higgs is due to a smaller coupling of SM fermions to the KK gluon for the bulk Higgs case, i.e., the zero-mode fermions being localized a bit farther from the TeV brane (where gauge KK modes are localized), than for the brane-localized Higgs case. The crucial point is that, even with this shift of zero-mode fermion profiles relative to the brane-localized Higgs case, the bulk Higgs set-up can maintain the *same* (i.e., SM) value of the zero-mode Yukawa (for the *same* KK Yukawa) as in brane-localized Higgs case. Here, we use the result (explained above) that the ratio of zero-mode to KK Yukawa couplings (denoted by a above) is larger for the bulk Higgs case than for brane-localized Higgs (for fixed fermion profiles).

We remind the reader that we are *not* considering models where Higgs is the 5^{th} component of $5D$ gauge field here. In the Higgs-as-A_5 model, the SM Higgs also has a profile which is peaked near the TeV brane *in a specific gauge* [27]. However, for this model, it was shown in reference [14] that the lower limit on the KK mass scale is $\sim$ 10 TeV for the choices $g_5^{QCD}\sqrt{k} \sim 3$ and $g_5^{EW}\sqrt{k}$ (which is the "effective" $5D$ Yukawa) ~ 6. For larger $g_5^{QCD}\sqrt{k}$ and/or smaller $g_5^{EW}\sqrt{k}$, the bound on KK scale is higher.

E.4 Perturbativity limit on size of KK Yukawa

Finally, we wish to illustrate why ϵ_K *by itself* might allow *a few*, say, ~ 3 TeV KK scale, even with *anarchy* in $5D$ flavor parameters, i.e., mixing angles of size as in Eq. (20). The point is that the bound on KK scale from ϵ_K depends on size of KK Yukawa as seen in Eq. (103). Instead of using $b \to s\gamma$ in order to constrain Y_{KK} (as we did for the two-site model), we can use perturbativity of the $5D$ theory.

Proceeding in the same way as for the gluon coupling, we can estimate N_{KK} from the loop expansion parameter associated with the Yukawa coupling being ~ 1. For example, we can compare the one-loop correction to the tree-level value of the coupling of Higgs to two KK fermions from this coupling itself (there are no color or helicity factors here). For *brane*-localized Higgs, we get

$$\frac{Y_{KK}^{brane\ 2}}{16\pi^2} N_{KK}^2 \quad \sim \quad 1 \tag{104}$$

where N_{KK}^2 (i.e., *double* KK sum) in this loop diagram follows from absence of KK number conservation at the Higgs vertices in the brane-localized Higgs case. One can also derive such growth of the loop expansion parameter with N_{KK} from dimensional analysis, namely, $[Y_5^{brane}] = -1$ such that the $5D$ loop expansion parameter is $\sim Y_5^{brane\ 2} E^2 / \left(16\pi^2\right)$. So, for the brane-localized Higgs case, we get $Y_{KK}^{brane} \sim 4\pi / N_{KK}$ and the choice of $Y_{KK} \sim 6$ (i.e., $Y_5^{brane} k \sim 3$) in references [14, 15] for brane Higgs corresponds to $N_{KK} \sim 2$.

On the other hand, the loop expansion parameter for the *bulk* Higgs case is

$$\frac{Y_{KK}^{bulk\ 2}}{16\pi^2} N_{KK} \quad \sim \quad 1 \tag{105}$$

where the *single* power of N_{KK} follows from the single KK sum due to KK number conservation at Higgs vertices for the bulk Higgs case. Equivalently, we can use dimensional analysis, i.e., $[Y_5^{bulk}] = -1/2$ so that the $5D$ loop expansion parameter $\sim Y_5^{bulk\ 2} E / \left(16\pi^2\right)$ just like for $5D$ gauge theory. Hence, we have for bulk Higgs case, $Y_{KK}^{bulk} \sim 4\pi/\sqrt{N_{KK}}$, i.e.,

- for same N_{KK}, we find that Y_{KK} can be larger for bulk Higgs by $\sim \sqrt{N_{KK}}$ than for the brane-localized Higgs case. Thus the KK mass bound can be lowered even further (*beyond* the point related to the factor a discussed above) as seen from Eq (103): see also discussion in [16].

And, in particular,

- we get $Y_{KK}^{bulk} \sim 6\sqrt{2}$ for $N_{KK} \sim 2$ (same as the choice made in references [14, 15]) so that choosing in addition the Higgs profile with $\beta \sim 0$ (so that $a \sim 1.5$) and $g_* \sim 3$, we see from Eq. (103) that $M_{KK} \sim 2.6$ TeV might be allowed by ϵ_K constraint.

However, such a low KK scale and large Y_{KK} in the $5D$ model will most likely be very strongly constrained by BR $(b \to s\gamma)$ just as in the case of the two-site model. Note that the bulk Higgs couplings other than $Y_{0,\,KK}$ – for example the mixed (i.e., zero-KK fermion) ones – might not *exactly* mimic the corresponding ones in the two-site model so that our results for $b \to s\gamma$ in the two-site model cannot be directly used for the $5D$ model[18]. A detailed calculation of $b \to s\gamma$ for the $5D$ model is beyond the scope of this work.

References

[1] H. Davoudiasl, J. L. Hewett and T. G. Rizzo, Phys. Lett. B **473**, 43 (2000) [arXiv:hep-ph/9911262]; A. Pomarol, Phys. Lett. B **486**, 153 (2000) [arXiv:hep-ph/9911294]; S. Chang, J. Hisano, H. Nakano, N. Okada and M. Yamaguchi, Phys. Rev. D **62**, 084025 (2000) [arXiv:hep-ph/9912498].

[2] Y. Grossman and M. Neubert, Phys. Lett. B **474**, 361 (2000) [arXiv:hep-ph/9912408].

[3] T. Gherghetta and A. Pomarol, Nucl. Phys. B **586**, 141 (2000) [arXiv:hep-ph/0003129].

[4] L. Randall and R. Sundrum, Phys. Rev. Lett. **83**, 3370 (1999) [arXiv:hep-ph/9905221].

[5] K. Agashe, R. Contino and R. Sundrum, Phys. Rev. Lett. **95**, 171804 (2005) [arXiv:hep-ph/0502222].

[6] K. Agashe and G. Servant, Phys. Rev. Lett. **93**, 231805 (2004) [arXiv:hep-ph/0403143] and JCAP **0502**, 002 (2005) [arXiv:hep-ph/0411254].

[7] K. Agashe, A. Delgado, M. J. May and R. Sundrum, JHEP **0308**, 050 (2003) [arXiv:hep-ph/0308036].

[8] K. Agashe, R. Contino and A. Pomarol, Nucl. Phys. B **719**, 165 (2005) [arXiv:hep-ph/0412089];

[9] K. Agashe and R. Contino, Nucl. Phys. B **742**, 59 (2006) [arXiv:hep-ph/0510164]; M. Carena, E. Ponton, J. Santiago and C. E. M. Wagner, Nucl. Phys. B **759**, 202 (2006) [arXiv:hep-ph/0607106] and arXiv:hep-ph/0701055; R. Contino, L. Da Rold and A. Pomarol, Phys. Rev. D **75**, 055014 (2007) [arXiv:hep-ph/0612048]; A. D. Medina, N. R. Shah and C. E. M. Wagner, Phys. Rev. D **76**, 095010 (2007) [arXiv:0706.1281 [hep-ph]]; C. Bouchart and G. Moreau, arXiv:0807.4461 [hep-ph].

---

[18] Of course, the amplitude for $b \to \gamma$ in the $5D$ model is expected to be of similar size to (i.e., differing only by $\sim O(1)$ factors from) that in the two-site model.

[10] K. Agashe, R. Contino, L. Da Rold and A. Pomarol, Phys. Lett. B **641**, 62 (2006) [arXiv:hep-ph/0605341].

[11] A. Delgado, A. Pomarol and M. Quiros, JHEP **0001**, 030 (2000) [arXiv:hep-ph/9911252].

[12] S. J. Huber and Q. Shafi, Phys. Lett. B **498**, 256 (2001) [arXiv:hep-ph/0010195].

[13] K. Agashe, G. Perez and A. Soni, Phys. Rev. D **71**, 016002 (2005) [arXiv:hep-ph/0408134].

[14] C. Csaki, A. Falkowski and A. Weiler, JHEP **0809**, 008 (2008) [arXiv:0804.1954 [hep-ph]].

[15] M. Blanke, A. J. Buras, B. Duling, S. Gori and A. Weiler, arXiv:0809.1073 [hep-ph].

[16] A. L. Fitzpatrick, G. Perez and L. Randall, arXiv:0710.1869 [hep-ph].

[17] S. Davidson, G. Isidori and S. Uhlig, Phys. Lett. B **663**, 73 (2008) [arXiv:0711.3376 [hep-ph]];

[18] G. Cacciapaglia, C. Csaki, J. Galloway, G. Marandella, J. Terning and A. Weiler, JHEP **0804**, 006 (2008) [arXiv:0709.1714 [hep-ph]]; M. C. Chen and H. B. Yu, arXiv:0804.2503 [hep-ph]; G. Perez and L. Randall, arXiv:0805.4652 [hep-ph]; C. Csaki, C. Delaunay, C. Grojean and Y. Grossman, arXiv:0806.0356 [hep-ph]; J. Santiago, arXiv:0806.1230 [hep-ph]; C. Csaki, Y. Grossman, G. Perez, Z. Surujon and A. Weiler, to appear.

[19] C. Csaki, A. Falkowski and A. Weiler, arXiv:0806.3757 [hep-ph].

[20] For studies with $\sim$ 10 TeV KK masses, see S. J. Huber and Q. Shafi, Phys. Lett. B **512**, 365 (2001) [arXiv:hep-ph/0104293]; S. J. Huber, Nucl. Phys. B **666**, 269 (2003) [arXiv:hep-ph/0303183]; S. Khalil and R. Mohapatra, Nucl. Phys. B **695**, 313 (2004) [arXiv:hep-ph/0402225].

[21] G. Burdman, Phys. Lett. B **590**, 86 (2004) [arXiv:hep-ph/0310144]; G. Moreau and J. I. Silva-Marcos, JHEP **0603**, 090 (2006) [arXiv:hep-ph/0602155]; K. Agashe, G. Perez and A. Soni, Phys. Rev. D **75**, 015002 (2007) [arXiv:hep-ph/0606293]; S. Chang, C. S. Kim and J. Song, JHEP **0702**, 087 (2007) [arXiv:hep-ph/0607313] and Phys. Rev. D **77**, 075001 (2008) [arXiv:0712.0207 [hep-ph]]; P. M. Aquino, G. Burdman and O. J. P. Eboli, Phys. Rev. Lett. **98**, 131601 (2007) [arXiv:hep-ph/0612055]; W. F. Chang, J. N. Ng and J. M. S. Wu, arXiv:0806.0667 [hep-ph] and arXiv:0809.1390 [hep-ph].

[22] K. Agashe, G. Perez and A. Soni, Phys. Rev. Lett. **93**, 201804 (2004) [arXiv:hep-ph/0406101].

[23] K. Agashe, A. E. Blechman and F. Petriello, Phys. Rev. D **74**, 053011 (2006) [arXiv:hep-ph/0606021].

[24] S. Casagrande, F. Goertz, U. Haisch, M. Neubert and T. Pfoh, arXiv:0807.4937 [hep-ph].

[25] H. Davoudiasl, B. Lillie and T. G. Rizzo, JHEP **0608**, 042 (2006) [arXiv:hep-ph/0508279]; M. Piai, arXiv:hep-ph/0608241; J. Hirn and V. Sanz, JHEP **0703**, 100 (2007) [arXiv:hep-ph/0612239]; C. D. Carone, J. Erlich and J. A. Tan, Phys. Rev. D **75**, 075005 (2007) [arXiv:hep-ph/0612242].

[26] G. Cacciapaglia, C. Csaki, G. Marandella and J. Terning, JHEP **0702**, 036 (2007) [arXiv:hep-ph/0611358].

[27] R. Contino, Y. Nomura and A. Pomarol, Nucl. Phys. B **671**, 148 (2003) [arXiv:hep-ph/0306259].

[28] P. McGuirk, G. Shiu and K. M. Zurek, JHEP **0803**, 012 (2008) [arXiv:0712.2264 [hep-ph]]; G. Shiu, B. Underwood, K. M. Zurek and D. G. E. Walker, Phys. Rev. Lett. **100**, 031601 (2008) [arXiv:0705.4097 [hep-ph]]; A. Falkowski and M. Perez-Victoria, arXiv:0806.1737 [hep-ph]; B. Batell, T. Gherghetta and D. Sword, arXiv:0808.3977 [hep-ph].

[29] H. Davoudiasl, J. L. Hewett and T. G. Rizzo, Phys. Rev. D **68**, 045002 (2003) [arXiv:hep-ph/0212279]; M. Carena, E. Ponton, T. M. P. Tait and C. E. M. Wagner, Phys. Rev. D **67**, 096006 (2003) [arXiv:hep-ph/0212307]; M. S. Carena, A. Delgado, E. Ponton, T. M. P. Tait and C. E. M. Wagner, Phys. Rev. D **68**, 035010 (2003) [arXiv:hep-ph/0305188]; M. S. Carena, A. Delgado, E. Ponton, T. M. P. Tait and C. E. M. Wagner, Phys. Rev. D **71**, 015010 (2005) [arXiv:hep-ph/0410344].

[30] R. Contino, T. Kramer, M. Son and R. Sundrum, JHEP **0705**, 074 (2007) [arXiv:hep-ph/0612180].

[31] N. Arkani-Hamed, A. G. Cohen and H. Georgi, Phys. Rev. Lett. **86**, 4757 (2001) [arXiv:hep-th/0104005]; C. T. Hill, S. Pokorski and J. Wang, Phys. Rev. D **64**, 105005 (2001) [arXiv:hep-th/0104035].

[32] J. M. Maldacena, Adv. Theor. Math. Phys. **2**, 231 (1998) [Int. J. Theor. Phys. **38**, 1113 (1999)] [arXiv:hep-th/9711200]; S. S. Gubser, I. R. Klebanov and A. M. Polyakov, Phys. Lett. B **428**, 105 (1998) [arXiv:hep-th/9802109]; E. Witten, Adv. Theor. Math. Phys. **2**, 253 (1998) [arXiv:hep-th/9802150].

[33] N. Arkani-Hamed, M. Porrati and L. Randall, JHEP **0108**, 017 (2001) [arXiv:hep-th/0012148]; R. Rattazzi and A. Zaffaroni, JHEP **0104**, 021 (2001) [arXiv:hep-th/0012248].

[34] A. J. Buras, published in ''Probing the Standard Model of Particle Interactions" (Les Houches lectures of 1997), arXiv:hep-ph/9806471.

[35] M. Bona *et al.* [UTfit Collaboration], JHEP **0803** (2008) 049 [arXiv:0707.0636 [hep-ph]].

[36] M. Misiak *et al.*, Phys. Rev. Lett. **98**, 022002 (2007) [arXiv:hep-ph/0609232].

[37] Heavy Flavor Averaging Group, http://www.slac.stanford.edu/xorg/hfag/rare/winter08/radll/btosg.pdf

[38] T. Huber, J. Phys. Conf. Ser. **110**, 052024 (2008) [arXiv:0712.3158 [hep-ph]].

[39] K. Agashe, A. Belyaev, T. Krupovnickas, G. Perez and J. Virzi, Phys. Rev. D **77**, 015003 (2008) [arXiv:hep-ph/0612015]; B. Lillie, L. Randall and L. T. Wang, JHEP **0709**, 074 (2007) [arXiv:hep-ph/0701166]; B. Lillie, J. Shu and T. M. P. Tait, Phys. Rev. D **76**, 115016 (2007) [arXiv:0706.3960 [hep-ph]]; A. Djouadi, G. Moreau and R. K. Singh, Nucl. Phys. B **797**, 1 (2008) [arXiv:0706.4191 [hep-ph]]; M. Guchait, F. Mahmoudi and K. Sridhar, Phys. Lett. B **666**, 347 (2008) [arXiv:0710.2234 [hep-ph]]; U. Baur and L. H. Orr, Phys. Rev. D **76**, 094012 (2007) [arXiv:0707.2066 [hep-ph]] and Phys. Rev. D **77**, 114001 (2008) [arXiv:0803.1160 [hep-ph]]; M. Carena, A. D. Medina, B. Panes, N. R. Shah and C. E. M. Wagner, Phys. Rev. D **77**, 076003 (2008) [arXiv:0712.0095 [hep-ph]].

[40] K. Agashe *et al.*, Phys. Rev. D **76**, 115015 (2007) [arXiv:0709.0007 [hep-ph]]; K. Agashe, S. Gopalakrishna, T. Han, G-Y. Huang and A. Soni, arXiv:0810.1497 [hep-ph].

[41] E. Lunghi and A. Soni, JHEP **0709**, 053 (2007) [arXiv:0707.0212 [hep-ph]]; E. Lunghi and A. Soni, Phys. Lett. B **666**, 162 (2008) [arXiv:0803.4340 [hep-ph]]; A. J. Buras and D. Guadagnoli, Phys. Rev. D **78**, 033005 (2008) [arXiv:0805.3887 [hep-ph]].

[42] M. Bona *et al.* [UTfit Collaboration], arXiv:0803.0659 [hep-ph].

[43] D. Atwood, M. Gronau and A. Soni, Phys. Rev. Lett. **79**, 185 (1997) [arXiv:hep-ph/9704272].

[44] Heavy Flavor Averaging Group, http://www.slac.stanford.edu/xorg/hfag/triangle/winter2008/index.shtml#bsgamma

[45] For applications to compact slice of AdS, see, for example, A. Lewandowski, M. J. May and R. Sundrum, Phys. Rev. D **67**, 024036 (2003) [arXiv:hep-th/0209050]; A. Lewandowski and M. Redi, Phys. Rev. D **68**, 044012 (2003) [arXiv:hep-th/0305013]; A. Lewandowski, Phys. Rev. D **71**, 024006 (2005) [arXiv:hep-th/0409192].

[46] A. Pomarol, Phys. Rev. Lett. **85**, 4004 (2000) [arXiv:hep-ph/0005293]; L. Randall and M. D. Schwartz, Phys. Rev. Lett. **88**, 081801 (2002) [arXiv:hep-th/0108115] and JHEP **0111**, 003 (2001) [arXiv:hep-th/0108114]; W. D. Goldberger and I. Z. Rothstein, Phys. Rev. Lett. **89**, 131601 (2002) [arXiv:hep-th/0204160]; Phys. Rev. D **68**, 125011 (2003) [arXiv:hep-th/0208060] and Phys. Rev. D **68**, 125012 (2003) [arXiv:hep-ph/0303158]; K. Agashe, A. Delgado and R. Sundrum, Nucl. Phys. B **643**, 172 (2002) [arXiv:hep-ph/0206099] and Annals Phys. **304**, 145 (2003) [arXiv:hep-ph/0212028]; R. Contino, P. Creminelli and E. Trincherini, JHEP **0210**, 029 (2002) [arXiv:hep-th/0208002].

[47] K. w. Choi and I. W. Kim, Phys. Rev. D **67**, 045005 (2003) [arXiv:hep-th/0208071].

[48] H. Davoudiasl, G. Perez and A. Soni, Phys. Lett. B **665**, 67 (2008) [arXiv:0802.0203 [hep-ph]].

[49] T. Appelquist, H. C. Cheng and B. A. Dobrescu, Phys. Rev. D **64**, 035002 (2001) [arXiv:hep-ph/0012100].

[50] K. Agashe, T. Okui and R. Sundrum, arXiv:0810.1277 [hep-ph].

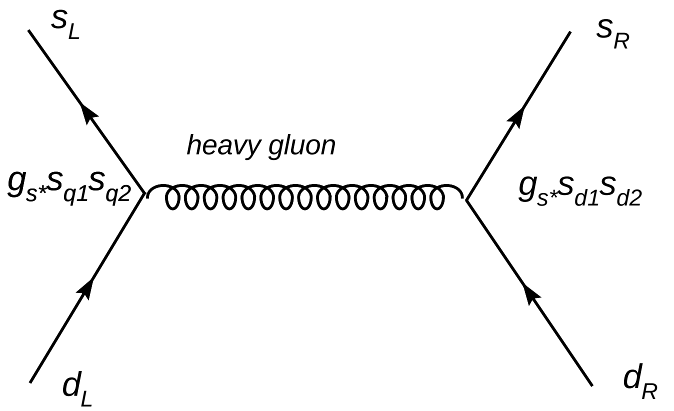

Figure 1: Feynman diagram for $\Delta S = 2$ process via heavy gluon exchange

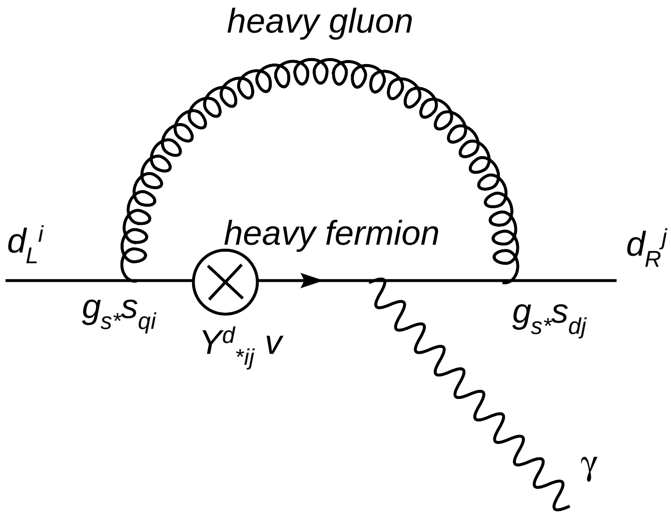

Figure 2: Feynman diagrams for b → s γ via heavy gluon and heavy fermions

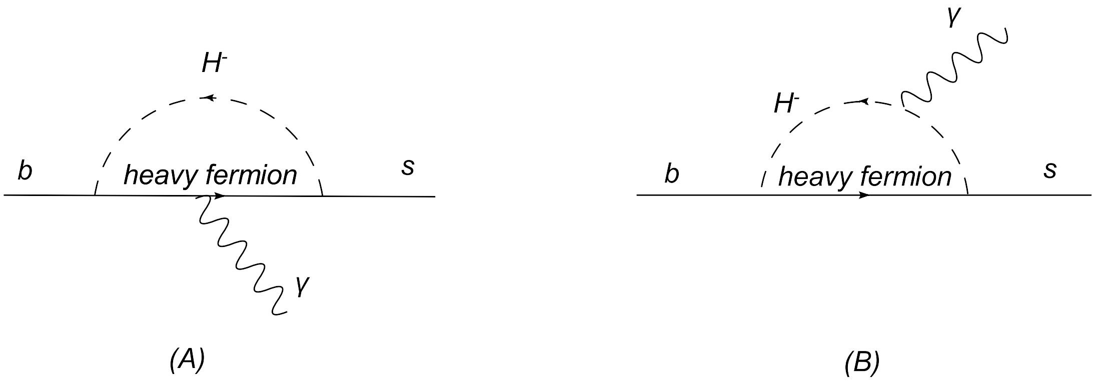

Figure 3: Feynman diagrams for b → s γ via charged Higgs

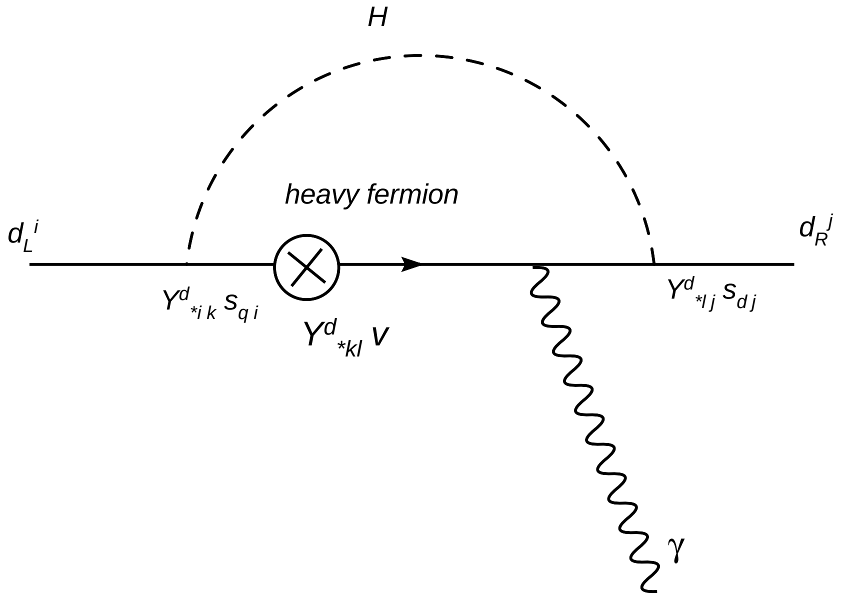

Figure 4: Feynman diagrams for b → s γ via Higgs using mass insertion

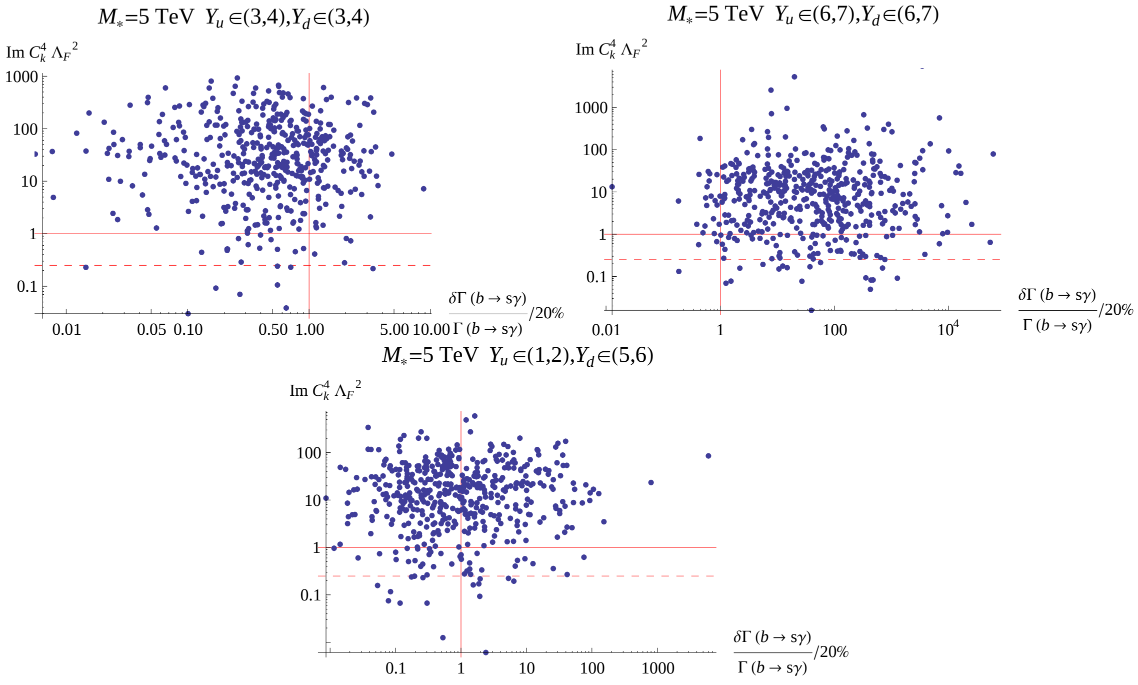

Figure 5: Scatter plot for shift in BR($b \to s\gamma$) and Im$\,(C_{4K})$ for $M_* = 5$ TeV, the composite site gauge coupling $g_{s*} = 3$ and different values of $Y_*^{u,d}$ (defined here as the geometric *mean* of the composite site Yukawa couplings $|Y_{*\,ij}^{u,d}|$). The allowed region is below and to the left of the (red) solid lines. For $g_{s*} = 6$, the allowed region is below the dashed line and to the left of the solid (red) line. (see discussion in section 6).

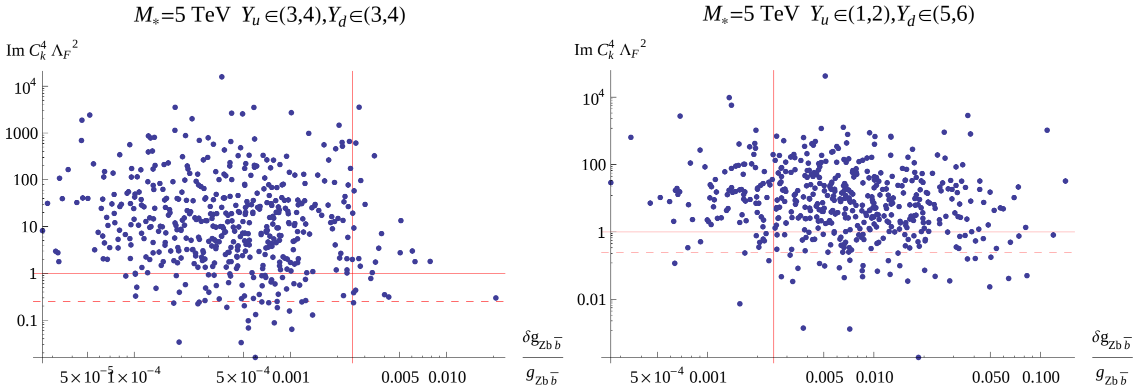

Figure 6: Scatter plot for $\delta g_{Z\bar{b}_L b_L}$ and $\mathrm{Im}\,(C_{4K})$ for $M_* = 5$ TeV, the composite site gauge coupling $g_{s*} = 3$ and for different values of $Y_*^{u,d}$ (defined here as the geometric *mean* of the composite site Yukawa couplings $|Y_{*\,ij}^{u,d}|$). The allowed region is below and to the left of the (red) solid lines. For $g_{s*} = 6$, the allowed region is below the dashed line and to the left of the solid (red) line. (see discussion in section 6).

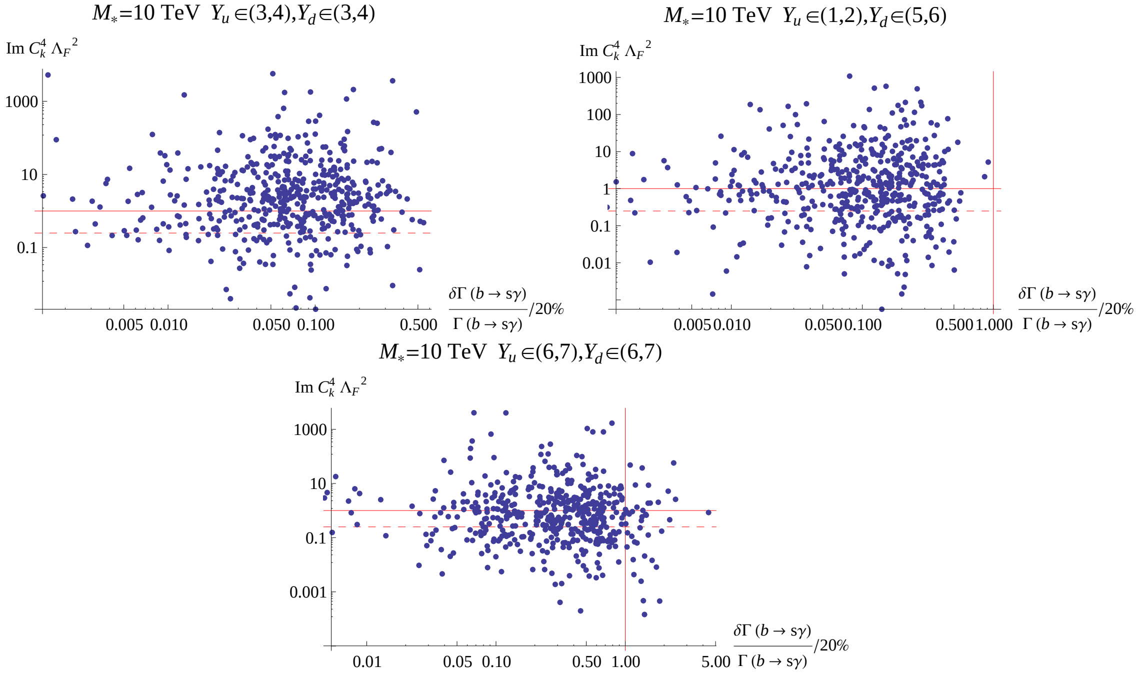

Figure 7: Same as Fig. 5, but with $M_* = 10$ TeV.

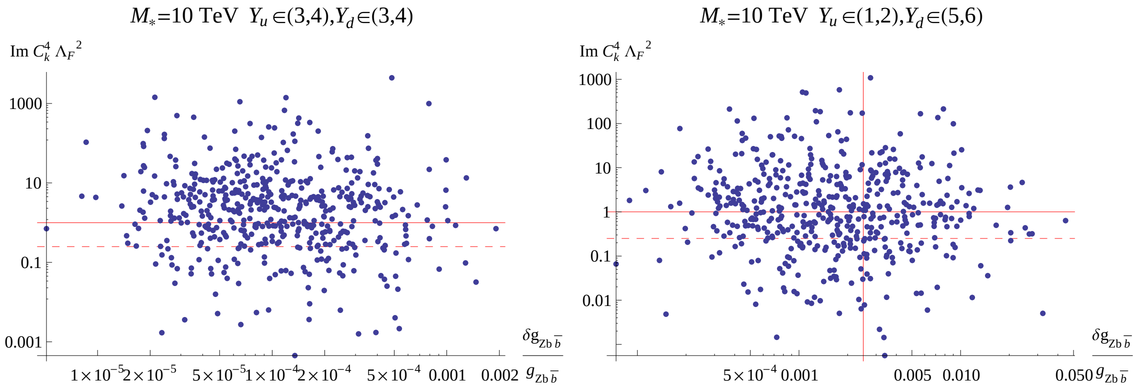

Figure 8: Same as Fig. 6, but with $M_* = 10$ TeV.

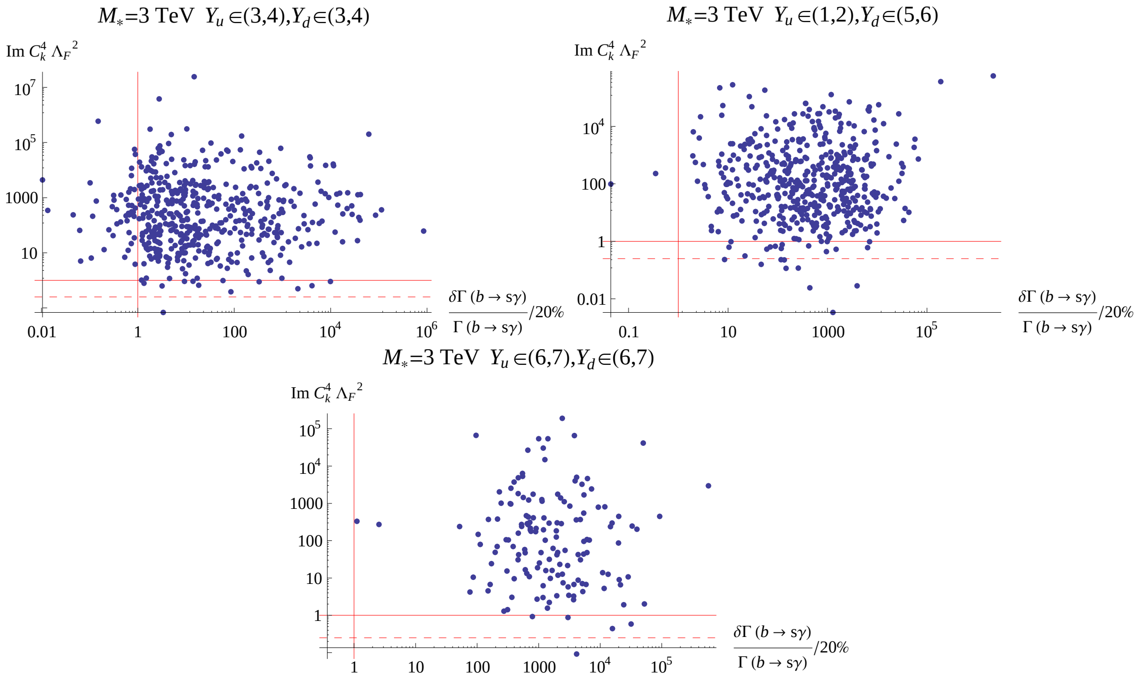

Figure 9: Same as Fig. 5, but with $M_* = 3$ TeV.

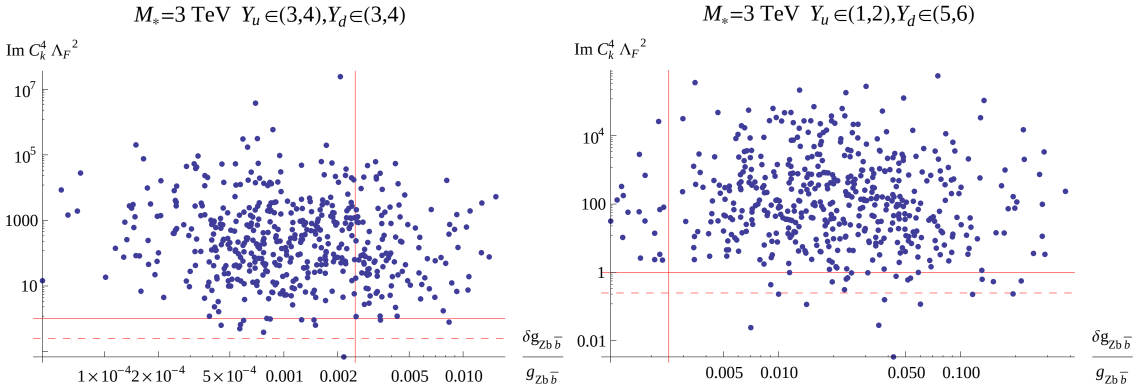
M_*=3 TeV $Y_u \in (3,4), Y_d \in (3,4)$

M_*=3 TeV $Y_u \in (1,2), Y_d \in (5,6)$

Figure 10: Same as Fig. 6, but with $M_* = 3$ TeV.